

Orbital Angular Momentum Small- x Evolution: Exact Results in the Large- N_c Limit

Brandon Manley*

Department of Physics, The Ohio State University, Columbus, OH 43210, USA

We construct an exact solution to the revised small- x orbital angular momentum (OAM) evolution equations derived in [1], based on an earlier work [2]. These equations are derived in the double logarithmic approximation (summing powers of $\alpha_s \ln^2(1/x)$ with α_s the strong coupling constant and x the Bjorken x variable) and the large- N_c limit, with N_c the number of quark colors. From our solution, we extract the small- x , large- N_c expressions of the quark and gluon OAM distributions. Additionally, we determine the large- N_c small- x asymptotics of the OAM distributions to be

$$L_{q+\bar{q}}(x, Q^2) \sim L_G(x, Q^2) \sim \Delta\Sigma(x, Q^2) \sim \Delta G(x, Q^2) \sim \left(\frac{1}{x}\right)^{\alpha_h},$$

with the intercept α_h the same as obtained in the small- x helicity evolution [3], which can be approximated as $\alpha_h \approx 3.66074\sqrt{\frac{\alpha_s N_c}{2\pi}}$. This result is in complete agreement with [4]. Additionally, we calculate the ratio of the quark and gluon OAM distributions to the flavor-singlet quark and gluon helicity parton distribution functions respectively in the small- x region.

CONTENTS

I. Introduction	1
II. Evolution equations for the moment amplitudes in the large- N_c limit	3
III. Solution of the moment amplitude evolution equations	7
IV. Summary of our solution and the small- x asymptotics	9
A. Summary of our solution	9
B. Small- x asymptotics of the OAM distributions	10
V. OAM to helicity PDF ratios	11
VI. Conclusions and outlook	15
Acknowledgments	16
A. Boundary conditions	16
B. Constraining a double Laplace image and the homogeneous neighbor functions	17
C. Exact expressions for the asymptotic OAM to helicity PDF ratios	19
References	25

I. INTRODUCTION

One of the most important open questions in hadronic physics is the proton spin puzzle [5–13]. The proton spin puzzle is best described by spin sum rules, due to Ji [14] and Jaffe and Manohar [15]. The latter reads

$$S_{q+\bar{q}} + L_{q+\bar{q}} + S_G + L_G = \frac{1}{2}, \quad (1)$$

* Email: manley.329@osu.edu

where $S_{q+\bar{q}}$ (S_G) is the quark (gluon) helicity contribution to the proton spin, and $L_{q+\bar{q}}$ (L_G) is the quark (gluon) contribution to the proton spin from the orbital angular momentum (OAM). The reader may find reviews of the proton spin puzzle in [6–9, 11, 12].

The helicity contributions can be expressed as integrals over the Bjorken x variable

$$S_{q+\bar{q}}(Q^2) = \frac{1}{2} \int_0^1 dx \Delta\Sigma(x, Q^2), \quad S_G(Q^2) = \int_0^1 dx \Delta G(x, Q^2), \quad (2)$$

where Q^2 is the renormalization scale and the flavor-singlet quark helicity parton distribution function (hPDF) is

$$\Delta\Sigma(x, Q^2) = \sum_{f=u,d,s,\dots} [\Delta q_f(x, Q^2) + \Delta \bar{q}_f(x, Q^2)]. \quad (3)$$

$\Delta q_f(x, Q^2)$ and $\Delta \bar{q}_f(x, Q^2)$ are respectively the quark and anti-quark hPDFs of a given flavor f . $\Delta G(x, Q^2)$ is the gluon hPDF. The current values of the spin carried by the quarks and gluons as extracted from experimental data are $S_{q+\bar{q}}(Q^2 = 10 \text{ GeV}^2) = 0.15 \div 0.20$ for $x \in [0.001, 1]$ and $S_G(Q^2 = 10 \text{ GeV}^2) = 0.13 \div 0.26$ for $x \in [0.05, 1]$ [6–9, 11, 12]. The fact that these two numbers sum to less than $1/2$ is the proton spin puzzle. The remaining spin could reside at lower values of x and/or the OAM contributions.

The OAM contributions can also be written as integrals over the Bjorken x variable [16–20],

$$L_{q+\bar{q}}(Q^2) = \int_0^1 dx L_{q+\bar{q}}(x, Q^2), \quad L_G(Q^2) = \int_0^1 dx L_G(x, Q^2). \quad (4)$$

Both the helicity PDFs and OAM distributions receive contributions from the small x region. This region is important to study because of the limited amount of data as well as the finite acceptance in x in any given experiment. Since x scales with the inverse of the center-of-mass energy squared, any experiment, even future experiments at the Electron-Ion Collider [6, 10, 11, 13], can only probe down to some $x_{\min} > 0$. Therefore, theoretical input is needed to constrain the net amount of spin for values of Bjorken $x < x_{\min}$.

The helicity PDFs, $\Delta\Sigma(x, Q^2)$ and $\Delta G(x, Q^2)$, have been well studied in recent years; they have been experimentally extracted in the accessible region of x and Q^2 [21–35]. The OAM contributions have been studied much less. Even though their evolution in Q^2 is known [17, 36], and there have been some proposals on how to access these distributions experimentally [37, 38], there is currently no experimental extraction of $L_{q+\bar{q}}(x, Q^2)$ and $L_G(x, Q^2)$. In order to fully understand the proton spin puzzle, more work is needed to understand the OAM distributions. As mentioned above, the small x region is particularly important for study.

In the helicity sector, a pioneering work by Bartels, Ermolaev, and Ryskin (BER) [39, 40] employed the infrared evolution equations (IREE) formalism [41–46] to study the hPDFs at small- x . These evolution equations were derived in the double-logarithmic approximation (DLA), which resums powers of $\alpha_s \ln^2(1/x)$, with α_s the strong coupling constant. The BER version of the IREE formalism was extended in [4] to study the OAM distributions at small- x .

Over the past decade, a new approach to helicity-dependent small- x evolution has been developed in [47–59]. This new approach is based on the s -channel/shock wave formalism previously developed for unpolarized scattering [60–72]. In unpolarized scattering, which dominates at high energies, the evolution in [60–72] is expressed in terms of infinite Wilson lines along the light-cone. This regime is known as the eikonal approximation. Helicity-dependent scattering is suppressed by one power of center-of-mass energy, and is known as the sub-eikonal approximation. This new approach, called the light-cone operator treatment (LCOT) in [59], utilizes sub-eikonal operators inserted between semi-infinite and finite light-cone Wilson lines.

Using the LCOT formalism, small x evolution equations were derived for the polarized dipole amplitudes, which are related to the hPDFs, in [47, 49, 52, 53] (KPS). The KPS equations were derived in the DLA. Recently, these equations received important corrections. It was discovered that additional sub-eikonal operators mix with the ones studied in the original KPS papers under evolution, and thus resulted in revised evolution equations [59] (KPS-CTT) (see [48] also). These revised evolution equations for the polarized dipole amplitudes were solved numerically in the large- N_c [59], and large- N_c & N_f [73] limits (where N_f is the number of quark flavors) as well as analytically in the large- N_c limit [3]. Additionally, the large- N_c & N_f solution has been used for a successful analysis of the polarized deep inelastic scattering (DIS) and semi-inclusive DIS (SIDIS) small- x data [74].

The small- x asymptotics of the hPDFs have been calculated by BER [40], and by solving the KPS-CTT equations [3, 59, 73]. It was shown that there is less than a 1% difference between the results for the intercept (power of x) in the large- N_c limit and less than a 3% difference between the results in the large- N_c & N_f limit. The origin of the discrepancy is speculated on in the Appendix of [3] (see also [49]). (Additionally, see [75, 76] for a discrepancy due to scheme dependence between the IREE and the small- x limit of the exact 3-loop calculations of spin-dependent DGLAP anomalous dimensions.)

The OAM distributions have also been studied in the LCOT framework. An analysis based on the KPS equations was done in [2], but did not include the corrections found in [59]. In [1], these corrections were accounted for and the OAM distributions were expressed in terms of the polarized dipole amplitudes and their first impact-parameter moments. These impact-parameter moments were dubbed the “moment amplitudes” in [1]. Novel evolution equations for the moment amplitudes based on the KPS-CTT equations were constructed and solved numerically in [1]. In the previous study based on the KPS equations, the small- x asymptotics of the OAM distributions were significantly different from each other. In the large- N_c limit, more than a 50% difference was found between the intercepts for the quark and gluon OAM distributions [2]. This result was consistent with the discrepancies between the helicity small x asymptotics obtained via the KPS equations and those obtained by BER. After including the corrections which resulted in the KPS-CTT evolution, it was found that the small x asymptotics of the OAM distributions agree with the result from [4], at least within the precision of the numerical solution in [1]. Furthermore, the ratios of the OAM distributions to the hPDFs were studied in [1] and compared to the results in [4]. Although the ratios in the gluon sector seemed consistent, a nearly 50% difference was found in the quark sector.

In this paper, we seek to elucidate the numerical findings of [1] by solving the large- N_c evolution equations for the moment amplitudes, Eq. (8) below, analytically. In Section II, we recall these evolution equations and the relations between the OAM distributions and the polarized dipole amplitudes and their first impact-parameter moments. We present the solution of the moment amplitude evolution equations in Section III, which is based on the double Laplace transform method of [3]. A summary of our solution and the resulting small- x asymptotics of the quark and gluon OAM distributions is presented in Section IV. Importantly, we find the OAM distributions have the same asymptotics as the hPDFs and the g_1 structure function, given in Eq. (40) as well as in the Abstract above. We trace the origin of this homogeneity to the mixing of the polarized dipole amplitudes with the moment amplitudes in the moment evolution equations.

In Section V, we use the solution of the moment amplitudes and the KPS-CTT equations to calculate the ratios of the OAM distributions to the hPDFs in the quark and gluon sectors analytically. We confirm and speculate on the discrepancy between the numerical result of [1] and the results in [4]. We conclude in Section VI.

II. EVOLUTION EQUATIONS FOR THE MOMENT AMPLITUDES IN THE LARGE- N_c LIMIT

The large- N_c DLA OAM evolution equations, as derived in [1], evolve the first impact-parameter moments of the polarized dipole amplitudes $G_{10}(zs)$ and $G_{10}^i(zs)$. The operator definitions of the polarized dipole amplitudes, given in [59], are in terms of infinite light-cone Wilson lines and polarized light-cone Wilson lines. The latter are expressed as sub-eikonal operators inserted between semi-infinite light-cone Wilson lines. The large- N_c DLA helicity evolution equations involve the impact-parameter integrated polarized dipole amplitudes, $G(x_{10}^2, zs)$ and $G_2(x_{10}^2, zs)$ defined by

$$\int d^2x_1 G_{10}(zs) = G(x_{10}^2, zs), \quad (5a)$$

$$\int d^2x_1 G_{10}^i(zs) = x_{10}^i G_1(x_{10}^2, zs) + \epsilon^{ij} x_{10}^j G_2(x_{10}^2, zs). \quad (5b)$$

As we will see below, $G_1(x_{10}^2, zs)$ does not contribute to the helicity PDFs or the evolution of $G(x_{10}^2, zs)$ and $G_2(x_{10}^2, zs)$. We use $\underline{x} = (x^1, x^2)$ to denote two-dimensional transverse vectors, and $\underline{x}_{ij} = \underline{x}_i - \underline{x}_j$ for $i, j = 0, 1, 2, \dots$ labeling the partons. The amplitudes above depend on $x_{10}^2 = |\underline{x}_{10}|^2$, the transverse size squared of the dipole. Additionally, the amplitudes depend on the center of mass energy between the original projectile and the target, s , multiplied by the smallest momentum fraction of the two partons making up the dipole, z .¹ The OAM distributions depend not only on $G(x_{10}^2, zs)$ and $G_2(x_{10}^2, zs)$, but also on the first impact-parameter moments of $G_{10}(zs)$ and $G_{10}^i(zs)$ defined as

$$\int d^2x_1 x_1^i G_{10}(zs) = x_{10}^i I_3(x_{10}^2, zs) + \dots, \quad (6a)$$

$$\int d^2x_1 x_1^i G_{10}^j(zs) = \epsilon^{ij} x_{10}^2 I_4(x_{10}^2, zs) + \epsilon^{ik} x_{10}^k x_{10}^j I_5(x_{10}^2, zs) + \epsilon^{jk} x_{10}^k x_{10}^i I_6(x_{10}^2, zs) + \dots, \quad (6b)$$

where the ellipses denote additional tensor structures that do not contribute to the OAM distributions. The amplitudes I_3, I_4, I_5 and I_6 were dubbed the “moment” amplitudes in [1]. The evolution of the moment amplitudes mixes them with $G(x_{10}^2, zs)$ and $G_2(x_{10}^2, zs)$ and was derived in [1].

¹ z is more aptly thought of as the parameter controlling the evolution of zs [47, 53, 58]. For instance, after a step of evolution involving a virtual correction, z could be smaller than either of the two longitudinal momentum fractions of the partons making up the dipole.

In addition to the amplitudes in Eqs. (5) and (6), the evolution for the moment amplitudes (as well the helicity evolution) depends on the so-called neighbor dipole amplitudes, denoted by $\Gamma_{10,21}(zs)$ and $\Gamma_{10,21}^i(zs)$, which are auxiliary amplitudes necessary to enforce lifetime ordering in the evolution [47]. Their operator definitions are the same as those for $G_{10}(zs)$ and $G_{10}^i(zs)$, except for a difference in the light-cone lifetime cutoff, which depends on the adjacent dipole size [53, 54, 59]. One can write decompositions analogous to Eqs. (5) and (6) for the neighbor amplitudes,

$$\int d^2 x_1 \Gamma_{10,21}(zs) = \Gamma(x_{10}^2, x_{21}^2, zs), \quad (7a)$$

$$\int d^2 x_1 \Gamma_{10,21}^i(zs) = \epsilon^{ij} x_{10}^j \Gamma_2(x_{10}^2, x_{21}^2, zs) + \dots, \quad (7b)$$

$$\int d^2 x_1 x_1^i \Gamma_{10,21}(zs) = x_{10}^i \Gamma_3(x_{10}^2, x_{21}^2, zs) + \dots, \quad (7c)$$

$$\int d^2 x_1 x_1^i \Gamma_{10,21}^j(zs) = \epsilon^{ij} x_{10}^2 \Gamma_4(x_{10}^2, x_{21}^2, zs) + \epsilon^{ik} x_{10}^k x_{10}^j \Gamma_5(x_{10}^2, x_{21}^2, zs) + \epsilon^{jk} x_{10}^k x_{10}^i \Gamma_6(x_{10}^2, x_{21}^2, zs) + \dots, \quad (7d)$$

where again the ellipses denote additional tensor structures that do not contribute to the helicity PDFs, OAM distributions or the evolution of the dipole and moment amplitudes. Neither the helicity PDFs nor the OAM distributions depend on the neighbor amplitudes directly. The neighbor amplitudes only contribute to the evolution of the dipole and moment amplitudes. As we will see below, the helicity PDFs and OAM distributions depend only on the polarized dipole and moment amplitudes.

The DLA evolution equations for the moment amplitudes in the large- N_c limit are [1]

$$\begin{aligned} \begin{pmatrix} I_3 \\ I_4 \\ I_5 \\ I_6 \end{pmatrix} (x_{10}^2, zs) &= \begin{pmatrix} I_3^{(0)} \\ I_4^{(0)} \\ I_5^{(0)} \\ I_6^{(0)} \end{pmatrix} (x_{10}^2, zs) \\ &+ \frac{\alpha_s N_c}{4\pi} \int_{\frac{1}{sx_{10}^2}}^z \frac{dz'}{z'} \int_{\frac{1}{z's}}^{x_{10}^2} \frac{dx_{21}^2}{x_{21}^2} \begin{pmatrix} 2\Gamma_3 - 4\Gamma_4 + 2\Gamma_5 + 6\Gamma_6 - 2\Gamma_2 \\ 0 \\ 0 \\ 0 \end{pmatrix} (x_{10}^2, x_{21}^2, z's) \\ &+ \frac{\alpha_s N_c}{4\pi} \int_{\frac{\Lambda^2}{s}}^z \frac{dz'}{z'} \int_{\max[x_{10}^2, \frac{1}{z's}]}^{\min[\frac{z'}{z'}, x_{10}^2, \frac{1}{\Lambda^2}]} \frac{dx_{21}^2}{x_{21}^2} \begin{pmatrix} 4 & -4 & 2 & 6 & -4 & -6 \\ 0 & 4 & 2 & -2 & 0 & 1 \\ -2 & 2 & -1 & -3 & 2 & 3 \\ 0 & 0 & 0 & 0 & 2 & 4 \end{pmatrix} \begin{pmatrix} I_3 \\ I_4 \\ I_5 \\ I_6 \\ G \\ G_2 \end{pmatrix} (x_{21}^2, z's), \end{aligned} \quad (8)$$

where the inhomogeneous terms are the initial conditions of the evolution. The DLA evolution equations for the neighbor moment amplitudes are [1]

$$\begin{aligned} \begin{pmatrix} \Gamma_3 \\ \Gamma_4 \\ \Gamma_5 \\ \Gamma_6 \end{pmatrix} (x_{10}^2, x_{21}^2, z's) &= \begin{pmatrix} \Gamma_3^{(0)} \\ \Gamma_4^{(0)} \\ \Gamma_5^{(0)} \\ \Gamma_6^{(0)} \end{pmatrix} (x_{10}^2, z's) \\ &+ \frac{\alpha_s N_c}{4\pi} \int_{\frac{1}{sx_{10}^2}}^{z'} \frac{dz''}{z''} \int_{\frac{1}{z''s}}^{\min[x_{10}^2, x_{21}^2, \frac{z'}{z''}]} \frac{dx_{32}^2}{x_{32}^2} \begin{pmatrix} 2\Gamma_3 - 4\Gamma_4 + 2\Gamma_5 + 6\Gamma_6 - 2\Gamma_2 \\ 0 \\ 0 \\ 0 \end{pmatrix} (x_{10}^2, x_{32}^2, z''s) \\ &+ \frac{\alpha_s N_c}{4\pi} \int_{\frac{\Lambda^2}{s}}^{z' \frac{x_{21}^2}{x_{10}^2}} \frac{dz''}{z''} \int_{\max[x_{10}^2, \frac{1}{z''s}]}^{\min[\frac{z'}{z''}, x_{21}^2, \frac{1}{\Lambda^2}]} \frac{dx_{32}^2}{x_{32}^2} \begin{pmatrix} 4 & -4 & 2 & 6 & -4 & -6 \\ 0 & 4 & 2 & -2 & 0 & 1 \\ -2 & 2 & -1 & -3 & 2 & 3 \\ 0 & 0 & 0 & 0 & 2 & 4 \end{pmatrix} \begin{pmatrix} I_3 \\ I_4 \\ I_5 \\ I_6 \\ G \\ G_2 \end{pmatrix} (x_{32}^2, z''s), \end{aligned} \quad (9)$$

where $\Gamma_p(x_{10}^2, x_{21}^2, z's)$ for $p = 2, 3, 4, 5, 6$ are only defined for $x_{10} \geq x_{21}$, and $1/\Lambda$ is an infrared (IR) cutoff for all dipole sizes.

The dipole amplitudes G and G_2 , in addition to the neighbor amplitude Γ_2 , appear explicitly in Eqs. (8) and (9). Therefore, to solve Eqs. (8) and (9), one needs to first solve the large- N_c helicity evolution equations, Eqs. (133) of [59], to obtain G, G_2 , and Γ_2 . This has been done in [3]. We will use their solution for G, G_2, Γ_2 below to solve Eqs. (8) and (9).

For brevity, we will use the following linear combination of amplitudes

$$\bar{I}_3(x_{10}^3, zs) \equiv I_3(x_{10}^2, zs) + 2I_5(x_{10}^2, zs), \quad (10a)$$

$$\bar{\Gamma}_3(x_{10}^2, x_{21}^2, z's) \equiv \Gamma_3(x_{10}^2, x_{21}^2, z's) + 2\Gamma_5(x_{10}^2, x_{21}^2, z's), \quad (10b)$$

in place of $I_3(x_{10}^2, zs)$ and $\Gamma_3(x_{10}^2, x_{21}^2, z's)$ in Eqs. (8) and (9). Additionally, to simplify the algebra and notation, we introduce vectorial notation for the moment amplitudes appearing in Eqs. (6b) and (7d)

$$\vec{I}(x_{10}^2, zs) \equiv (I_4(x_{10}^2, zs), I_5(x_{10}^2, zs), I_6(x_{10}^2, zs)), \quad (11a)$$

$$\vec{\Gamma}(x_{10}^2, x_{21}^2, z's) \equiv (\Gamma_4(x_{10}^2, x_{21}^2, z's), \Gamma_5(x_{10}^2, x_{21}^2, z's), \Gamma_6(x_{10}^2, x_{21}^2, z's)). \quad (11b)$$

We may also express the initial conditions for the amplitudes in Eq. (11a) in a similar vector notation

$$\vec{I}^{(0)}(x_{10}^2, zs) \equiv (I_4^{(0)}(x_{10}^2, zs), I_5^{(0)}(x_{10}^2, zs), I_6^{(0)}(x_{10}^2, zs)). \quad (12)$$

Finally, it is more useful to work in terms of the rescaled variables [50, 55, 59]

$$\eta = \sqrt{\frac{\alpha_s N_c}{2\pi}} \ln \frac{zs}{\Lambda^2}, \quad \eta' = \sqrt{\frac{\alpha_s N_c}{2\pi}} \ln \frac{z's}{\Lambda^2}, \quad \eta'' = \sqrt{\frac{\alpha_s N_c}{2\pi}} \ln \frac{z''s}{\Lambda^2}, \quad (13a)$$

$$s_{10} = \sqrt{\frac{\alpha_s N_c}{2\pi}} \ln \frac{1}{x_{10}^2 \Lambda^2}, \quad s_{21} = \sqrt{\frac{\alpha_s N_c}{2\pi}} \ln \frac{1}{x_{21}^2 \Lambda^2}, \quad s_{32} = \sqrt{\frac{\alpha_s N_c}{2\pi}} \ln \frac{1}{x_{32}^2 \Lambda^2}. \quad (13b)$$

Utilizing Eqs. (10)-(13) in Eqs. (8) and (9), we may write the moment amplitude and neighbor evolution equations as

$$\bar{I}_3(s_{10}, \eta) = \bar{I}_3^{(0)}(s_{10}, \eta) + \int_{s_{10}}^{\eta} d\eta' \int_{s_{10}}^{\eta'} ds_{21} \left[\bar{\Gamma}_3(s_{10}, s_{21}, \eta') - \Gamma_2(s_{10}, s_{21}, \eta') + \vec{V}_{UV} \cdot \vec{\Gamma}(s_{10}, s_{21}, \eta') \right], \quad (14a)$$

$$\begin{aligned} \vec{I}(s_{10}, \eta) = \vec{I}^{(0)}(s_{10}, \eta) + \frac{1}{2} \int_0^{s_{10}} ds_{21} \int_{s_{21}}^{\eta - s_{10} + s_{21}} d\eta' \left[\bar{I}_3(s_{21}, \eta') \vec{V}_{I_3} + G(s_{21}, \eta') \vec{V}_G \right. \\ \left. + G_2(s_{21}, \eta') \vec{V}_{G_2} + M_{IR} \vec{I}(s_{21}, \eta') \right], \end{aligned} \quad (14b)$$

$$\begin{aligned} \bar{\Gamma}_3(s_{10}, s_{21}, \eta') = \bar{\Gamma}_3^{(0)}(s_{10}, \eta') + \int_{s_{10}}^{\eta'} d\eta'' \int_{\max[s_{10}, s_{21} + \eta'' - \eta']}^{\eta''} ds_{32} \left[\bar{\Gamma}_3(s_{10}, s_{32}, \eta'') - \Gamma_2(s_{10}, s_{32}, \eta'') \right. \\ \left. + \vec{V}_{UV} \cdot \vec{\Gamma}(s_{10}, s_{32}, \eta'') \right], \end{aligned} \quad (14c)$$

$$\begin{aligned} \vec{\Gamma}(s_{10}, s_{21}, \eta') = \vec{I}^{(0)}(s_{10}, \eta') + \frac{1}{2} \int_0^{s_{10}} ds_{32} \int_{s_{32}}^{\eta' - s_{21} + s_{32}} d\eta'' \left[\bar{I}_3(s_{32}, \eta'') \vec{V}_{I_3} + G(s_{32}, \eta'') \vec{V}_G \right. \\ \left. + G_2(s_{32}, \eta'') \vec{V}_{G_2} + M_{IR} \vec{I}(s_{32}, \eta'') \right], \end{aligned} \quad (14d)$$

where $0 \leq s_{10} \leq s_{21} \leq \eta'$, and we have changed the order of integration in the third lines of Eqs. (8) and (9). Additionally, we have defined

$$\vec{V}_{UV} \equiv (-2, -1, 3), \quad (15a)$$

$$\vec{V}_{I_3} \equiv (0, -2, 0), \quad (15b)$$

$$\vec{V}_G \equiv (0, 2, 2), \quad (15c)$$

$$\vec{V}_{G_2} \equiv (1, 3, 4), \quad (15d)$$

$$M_{\text{IR}} \equiv \begin{pmatrix} 4 & 2 & -2 \\ 2 & -1 & -3 \\ 0 & 0 & 0 \end{pmatrix}. \quad (15e)$$

The task is now to solve Eqs. (14). Furthermore, since the moment equations do not close on their own as mentioned above, we will need the solution for G, G_2 and Γ_2 from [3]. This solution is expressed in double Laplace transforms, and reads (see Eqs. (53) and (54) of [3])

$$G_2(s_{10}, \eta) = \int \frac{d\omega}{2\pi i} \int \frac{d\gamma}{2\pi i} e^{\omega(\eta-s_{10})+\gamma s_{10}} G_{2\omega\gamma}, \quad (16a)$$

$$G(s_{10}, \eta) = \int \frac{d\omega}{2\pi i} \int \frac{d\gamma}{2\pi i} e^{\omega(\eta-s_{10})+\gamma s_{10}} G_{\omega\gamma}, \quad (16b)$$

$$\Gamma_2(s_{10}, s_{21}, \eta') = \int \frac{d\omega}{2\pi i} \int \frac{d\gamma}{2\pi i} \left[e^{\omega(\eta'-s_{21})+\gamma s_{10}} \left(G_{2\omega\gamma} - G_{2\omega\gamma}^{(0)} \right) + e^{\omega(\eta'-s_{10})+\gamma s_{10}} G_{2\omega\gamma}^{(0)} \right], \quad (16c)$$

where the double Laplace images are

$$G_{2\omega\gamma} = G_{2\omega\gamma}^{(0)} + \frac{2(\gamma - \delta_\omega^+) \left(G_{\delta_\omega^+ \gamma}^{(0)} + 2G_{2\delta_\omega^+ \gamma}^{(0)} \right) - 2(\gamma_\omega^+ - \delta_\omega^+) \left(G_{\delta_\omega^+ \gamma_\omega^+}^{(0)} + 2G_{2\delta_\omega^+ \gamma_\omega^+}^{(0)} \right) + 8\delta_\omega^- \left(G_{2\omega\gamma}^{(0)} - G_{2\omega\gamma_\omega^+}^{(0)} \right)}{\omega(\gamma - \gamma_\omega^-)(\gamma - \gamma_\omega^+)}, \quad (17a)$$

$$G_{\omega\gamma} = \frac{1}{2}\omega\gamma(G_{2\omega\gamma} - G_{2\omega\gamma}^{(0)}) - 2G_{2\omega\gamma}. \quad (17b)$$

Here, the initial conditions of the helicity evolution have also been expressed in terms of double Laplace transforms

$$G^{(0)}(s_{10}, \eta) = \int \frac{d\omega}{2\pi i} \int \frac{d\gamma}{2\pi i} e^{\omega(\eta-s_{10})+\gamma s_{10}} G_{\omega\gamma}^{(0)}, \quad (18a)$$

$$G_2^{(0)}(s_{10}, \eta) = \int \frac{d\omega}{2\pi i} \int \frac{d\gamma}{2\pi i} e^{\omega(\eta-s_{10})+\gamma s_{10}} G_{2\omega\gamma}^{(0)}, \quad (18b)$$

and, following [3], we have also defined

$$\delta_\omega^\pm \equiv \frac{\omega}{2} \left[1 \pm \sqrt{1 - \frac{4}{\omega^2}} \right], \quad (19a)$$

$$\gamma_\omega^\pm \equiv \frac{\omega}{2} \left[1 \pm \sqrt{1 - \frac{16}{\omega^2} \sqrt{1 - \frac{4}{\omega^2}}} \right]. \quad (19b)$$

As usual, the contours in Eqs. (16) and (18) run parallel to the imaginary axis to the right of all the singularities of the integrands. Note, for the contours in Eqs. (16) and (18), $\text{Re } \omega > \text{Re } \gamma$ [3].

The solution of Eqs. (14), along with Eqs. (16), will give us both the OAM distributions and helicity PDFs at small- x and large- N_c , by employing the following relations derived in [1, 2, 59]

$$L_{q+\bar{q}}(x, Q^2) = \frac{N_f}{\alpha_s \pi^2} \int_0^{\sqrt{\alpha_s} \ln \frac{Q^2}{x\Lambda^2}} d\eta \int_{\max[\eta - \sqrt{\alpha_s} \ln \frac{1}{x}, 0]}^\eta ds_{10} \left[G(s_{10}, \eta) - 3G_2(s_{10}, \eta) \right. \\ \left. - \bar{I}_3(s_{10}, \eta) + (\vec{V}_{\text{UV}} - 2\vec{V}_{I_3}) \cdot \vec{I}(s_{10}, \eta) \right], \quad (20a)$$

$$L_G(x, Q^2) = -\frac{2N_c}{\alpha_s \pi^2} \left(2\vec{V}_G + V_{\bar{I}_3} - \vec{V}_{\text{UV}} \right) \cdot \vec{I} \left(s_{10} = \sqrt{\alpha_s} \ln \frac{Q^2}{\Lambda^2}, \eta = \sqrt{\alpha_s} \ln \frac{Q^2}{x\Lambda^2} \right), \quad (20b)$$

$$\Delta\Sigma(x, Q^2) = -\frac{N_f}{\alpha_s \pi^2} \int_0^{\sqrt{\alpha_s} \ln \frac{Q^2}{x\Lambda^2}} d\eta \int_{\max[\eta - \sqrt{\alpha_s} \ln \frac{1}{x}, 0]}^\eta ds_{10} \left[G(s_{10}, \eta) + 2G_2(s_{10}, \eta) \right], \quad (20c)$$

$$\Delta G(x, Q^2) = \frac{2N_c}{\alpha_s \pi^2} G_2 \left(s_{10} = \sqrt{\bar{\alpha}_s} \ln \frac{Q^2}{\Lambda^2}, \eta = \sqrt{\bar{\alpha}_s} \ln \frac{Q^2}{x\Lambda^2} \right), \quad (20d)$$

where we have defined $\bar{\alpha}_s = \frac{\alpha_s N_c}{2\pi}$. Here we have assumed all flavors contribute equally so that summing over flavors results in a factor of N_f in Eqs. (20a) and (20c). This assumption will need to be revised for phenomenology, where G and I_3 would depend on flavor (see [74] for example). Note we have neglected the derivatives from Eq. (36) of [1], and Eq. (42) of [59]. Such derivatives remove one logarithm of energy and are therefore outside of our DLA approximation.

III. SOLUTION OF THE MOMENT AMPLITUDE EVOLUTION EQUATIONS

Inspired by the success of the double Laplace transform method used to solve the helicity evolution equations [3] (see also [51]), we also use double inverse Laplace representations here to solve Eqs. (14). To start, let us write the moment amplitudes, $\bar{I}_3(s_{10}, \eta)$, $\vec{I}(s_{10}, \eta)$, and their inhomogeneous terms, $\bar{I}_3^{(0)}(s_{10}, \eta)$, $\vec{I}^{(0)}(s_{10}, \eta)$, as

$$\bar{I}_3(s_{10}, \eta) = \int \frac{d\omega}{2\pi i} \int \frac{d\gamma}{2\pi i} e^{\omega(\eta-s_{10})+\gamma s_{10}} \bar{I}_{3\omega\gamma}, \quad (21a)$$

$$\bar{I}_3^{(0)}(s_{10}, \eta) = \int \frac{d\omega}{2\pi i} \int \frac{d\gamma}{2\pi i} e^{\omega(\eta-s_{10})+\gamma s_{10}} \bar{I}_{3\omega\gamma}^{(0)}, \quad (21b)$$

$$\vec{I}(s_{10}, \eta) = \int \frac{d\omega}{2\pi i} \int \frac{d\gamma}{2\pi i} e^{\omega(\eta-s_{10})+\gamma s_{10}} \vec{I}_{\omega\gamma}, \quad (21c)$$

$$\vec{I}^{(0)}(s_{10}, \eta) = \int \frac{d\omega}{2\pi i} \int \frac{d\gamma}{2\pi i} e^{\omega(\eta-s_{10})+\gamma s_{10}} \vec{I}_{\omega\gamma}^{(0)}. \quad (21d)$$

As mentioned above, we take the contours to the right of all the singularities of the integrands in Eqs. (21). Using Eqs. (21), we will solve Eqs. (14b) and (14d) first. To start, we can relate the different double Laplace images in Eqs. (21) by using them in Eq. (14b). Doing the s_{21} and η' integrals, we get

$$\begin{aligned} \int \frac{d\omega}{2\pi i} \int \frac{d\gamma}{2\pi i} e^{\omega(\eta-s_{10})+\gamma s_{10}} \vec{I}_{\omega\gamma} &= \int \frac{d\omega}{2\pi i} \int \frac{d\gamma}{2\pi i} \frac{1}{\omega\gamma} e^{\omega(\eta-s_{10})+\gamma s_{10}} \vec{I}_{\omega\gamma}^{(0)} \\ &+ \frac{1}{2} \int \frac{d\omega}{2\pi i} \int \frac{d\gamma}{2\pi i} \frac{1}{\omega\gamma} \left(e^{\omega(\eta-s_{10})+\gamma s_{10}} - e^{\gamma s_{10}} - e^{\omega(\eta-s_{10})} + 1 \right) \left(\bar{I}_{3\omega\gamma} \vec{V}_{\bar{I}_3} + G_{\omega\gamma} \vec{V}_G + G_{2\omega\gamma} \vec{V}_{G_2} + M_{\text{IR}} \vec{I}_{\omega\gamma} \right). \end{aligned} \quad (22)$$

Treating $\eta - s_{10}$ and s_{10} as separate variables, we can perform the forward Laplace transforms in Eq. (22) to see

$$\vec{I}_{\omega\gamma} = \vec{I}_{\omega\gamma}^{(0)} + \frac{1}{2\omega\gamma} \left(\bar{I}_{3\omega\gamma} \vec{V}_{\bar{I}_3} + G_{\omega\gamma} \vec{V}_G + G_{2\omega\gamma} \vec{V}_{G_2} + M_{\text{IR}} \vec{I}_{\omega\gamma} \right), \quad (23)$$

or, solving for $\vec{I}_{\omega\gamma}$,

$$\vec{I}_{\omega\gamma} = (2\omega\gamma - M_{\text{IR}})^{-1} \left(2\omega\gamma \vec{I}_{\omega\gamma}^{(0)} + G_{\omega\gamma} \vec{V}_G + G_{2\omega\gamma} \vec{V}_{G_2} + \vec{V}_{\bar{I}_3} \bar{I}_{3\omega\gamma} \right). \quad (24)$$

Next, we observe the following scaling relation from Eqs. (14b) and (14d),

$$\vec{\Gamma}(s_{10}, s_{21}, \eta') - \vec{I}^{(0)}(s_{10}, \eta') = \vec{I}(s_{10}, \eta = \eta' + s_{10} - s_{21}) - \vec{I}^{(0)}(s_{10}, \eta = \eta' + s_{10} - s_{21}), \quad (25)$$

which, after using Eqs. (21), gives

$$\vec{\Gamma}(s_{10}, s_{21}, \eta') = \int \frac{d\omega}{2\pi i} \int \frac{d\gamma}{2\pi i} \left[e^{\omega(\eta'-s_{21})+\gamma s_{10}} \left(\vec{I}_{\omega\gamma} - \vec{I}_{\omega\gamma}^{(0)} \right) + e^{\omega(\eta'-s_{10})+\gamma s_{10}} \vec{I}_{\omega\gamma}^{(0)} \right]. \quad (26)$$

Eqs. (14b) and (14d) have several boundary conditions that need to be satisfied. We explicitly check that our solution satisfies these boundary conditions in Appendix A. Therefore, we conclude Eqs. (14b) and (14d) are completely solved.

Let us now solve Eqs. (14a) and (14c). One can show, after differentiating Eq. (14c), that $\bar{\Gamma}_3$ obeys the following second-order partial differential equation

$$\left[\frac{\partial^2}{\partial s_{21}^2} + \frac{\partial^2}{\partial s_{21} \partial \eta'} + 1 \right] \bar{\Gamma}_3(s_{10}, s_{21}, \eta') = -\vec{V}_{\text{UV}} \cdot \vec{\Gamma}(s_{10}, s_{21}, \eta') + \Gamma_2(s_{10}, s_{21}, \eta'). \quad (27)$$

This differential equation has a homogeneous and a particular solution, which we label $\bar{\Gamma}_3^{(h)}$ and $\bar{\Gamma}_3^{(p)}$ respectively. The general solution of Eq. (27) would then be a sum of $\bar{\Gamma}_3^{(h)}$ and $\bar{\Gamma}_3^{(p)}$. Searching for a homogeneous solution of the form

$$\bar{\Gamma}_3^{(h)}(s_{10}, s_{21}, \eta') = \int \frac{d\omega}{2\pi i} e^{\omega(\eta' - s_{21}) + \gamma s_{21}} \bar{\Gamma}_{3\omega\gamma}(s_{10}) \quad (28)$$

yields the condition

$$\gamma^2 - \omega\gamma + 1 = 0. \quad (29)$$

The two solutions to Eq. (29) are $\gamma = \delta_\omega^+$ and $\gamma = \delta_\omega^-$ as defined above in Eq. (19a). The complete homogeneous solution to Eq. (27) is then

$$\bar{\Gamma}_3^{(h)}(s_{10}, s_{21}, \eta') = \int \frac{d\omega}{2\pi i} e^{\omega(\eta' - s_{21})} \left[e^{\delta_\omega^+ s_{21}} \bar{\Gamma}_{3\omega}^+(s_{10}) + e^{\delta_\omega^- s_{21}} \bar{\Gamma}_{3\omega}^-(s_{10}) \right], \quad (30)$$

where $\bar{\Gamma}_{3\omega}^\pm(s_{10})$ are arbitrary functions of s_{10} that can be constrained by boundary conditions. We explicitly determine these functions in Appendix B; they are listed in Eq. (B6) and below in Eq. (33a).

Using Eqs. (16c) and (26) in the right hand side of Eq. (27), one can easily show the particular solution is

$$\begin{aligned} \bar{\Gamma}_3^{(p)}(s_{10}, s_{21}, \eta') = \int \frac{d\omega}{2\pi i} \int \frac{d\gamma}{2\pi i} \left\{ e^{\omega(\eta' - s_{10}) + \gamma s_{10}} \left[G_{2\omega\gamma}^{(0)} - \vec{V}_{UV} \cdot \vec{I}_{\omega\gamma}^{(0)} \right] \right. \\ \left. + e^{\omega(\eta' - s_{21}) + \gamma s_{10}} \left[G_{2\omega\gamma} - G_{2\omega\gamma}^{(0)} - \vec{V}_{UV} \cdot \left(\vec{I}_{\omega\gamma} - \vec{I}_{\omega\gamma}^{(0)} \right) \right] \right\}. \end{aligned} \quad (31)$$

Via Eqs. (30) and (31), the general solution to Eq. (27) is

$$\begin{aligned} \bar{\Gamma}_3(s_{10}, s_{21}, \eta') = \int \frac{d\omega}{2\pi i} e^{\omega(\eta' - s_{21})} \left[\bar{\Gamma}_{3\omega}^+(s_{10}) e^{\delta_\omega^+ s_{21}} + \bar{\Gamma}_{3\omega}^-(s_{10}) e^{\delta_\omega^- s_{21}} \right] \\ + \int \frac{d\omega}{2\pi i} \int \frac{d\gamma}{2\pi i} \left\{ e^{\omega(\eta' - s_{10}) + \gamma s_{10}} \left[G_{2\omega\gamma}^{(0)} - \vec{V}_{UV} \cdot \vec{I}_{\omega\gamma}^{(0)} \right] \right. \\ \left. + e^{\omega(\eta' - s_{21}) + \gamma s_{10}} \left[G_{2\omega\gamma} - G_{2\omega\gamma}^{(0)} - \vec{V}_{UV} \cdot \left(\vec{I}_{\omega\gamma} - \vec{I}_{\omega\gamma}^{(0)} \right) \right] \right\}. \end{aligned} \quad (32)$$

To ensure consistency with the solution in Eq. (16), we also choose $\text{Re } \omega > \text{Re } \gamma$ here. As mentioned above, the functions $\bar{\Gamma}_{3\omega}^\pm(s_{10})$ and the image $\bar{I}_{3\omega\gamma}$ can be constrained via boundary conditions from Eqs. (14a) and (14c). This is done in Appendix B, and we simply quote the results here

$$\bar{\Gamma}_{3\omega}^\pm(s_{10}) = e^{-\delta_\omega^\pm s_{10}} \frac{\delta_\omega^\pm}{\delta_\omega^\pm - \delta_\omega^\mp} \int \frac{d\gamma}{2\pi i} e^{\gamma s_{10}} \left\{ (\omega \delta_\omega^\mp - 1) \left[G_{2\omega\gamma} - G_{2\omega\gamma}^{(0)} - \vec{V}_{UV} \cdot \left(\vec{I}_{\omega\gamma} - \vec{I}_{\omega\gamma}^{(0)} \right) \right] \right. \\ \left. - G_{2\omega\gamma}^{(0)} + \vec{V}_{UV} \cdot \vec{I}_{\omega\gamma}^{(0)} + \bar{I}_{3\omega\gamma} \right\}, \quad (33a)$$

$$\begin{aligned} \bar{I}_{3\omega\gamma} = \frac{\vec{V}_{UV} \cdot \left(\vec{I}_{\omega\gamma}^{(0)} - \vec{I}_{\delta_\omega^+ \gamma}^{(0)} \right) - G_{2\omega\gamma}^{(0)} + G_{2\delta_\omega^+ \gamma}^{(0)} - \bar{I}_{3\delta_\omega^+ \gamma}^{(0)}}{(\omega \delta_\omega^- - 1) \vec{V}_{UV} \cdot (2\omega\gamma - M_{\text{IR}})^{-1} \vec{V}_{\bar{I}_3} - 1} \\ + \frac{(\omega \delta_\omega^- - 1) \left[G_{2\omega\gamma} - G_{2\omega\gamma}^{(0)} + \vec{V}_{UV} \cdot \vec{I}_{\omega\gamma}^{(0)} - \vec{V}_{UV} \cdot (2\omega\gamma - M_{\text{IR}})^{-1} (2\omega\gamma \vec{I}_{\omega\gamma}^{(0)} + G_{\omega\gamma} \vec{V}_G + G_{2\omega\gamma} \vec{V}_{G_2}) \right]}{(\omega \delta_\omega^- - 1) \vec{V}_{UV} \cdot (2\omega\gamma - M_{\text{IR}})^{-1} \vec{V}_{\bar{I}_3} - 1}. \end{aligned} \quad (33b)$$

We have now completely solved Eqs. (14). That is, given the initial conditions to the evolution, $\bar{I}_3^{(0)}(s_{10}, \eta)$, $\vec{I}^{(0)}(s_{10}, \eta)$ as well as $G^0(s_{10}, \eta)$ and $G_2^{(0)}(s_{10}, \eta)$, we solve Eqs. (14) via Eqs. (21), (26), (23), (32), and (33).

IV. SUMMARY OF OUR SOLUTION AND THE SMALL- x ASYMPTOTICS

A. Summary of our solution

In the previous Section, we constructed an exact solution to Eqs. (14). We reiterate the solution here for convenience

$$\bar{I}_3(s_{10}, \eta) = \int \frac{d\gamma}{2\pi i} \int \frac{d\omega}{2\pi i} e^{\omega(\eta-s_{10})+\gamma s_{10}} \bar{I}_{3\omega\gamma}, \quad (34a)$$

$$\vec{I}(s_{10}, \eta) = \int \frac{d\gamma}{2\pi i} \int \frac{d\omega}{2\pi i} e^{\omega(\eta-s_{10})+\gamma s_{10}} (2\omega\gamma - M_{\text{IR}})^{-1} \left(2\omega\gamma \vec{I}_{\omega\gamma}^{(0)} + G_{\omega\gamma} \vec{V}_G + G_{2\omega\gamma} \vec{V}_{G_2} + \vec{V}_{\bar{I}_3} \bar{I}_{3\omega\gamma} \right), \quad (34b)$$

$$\bar{\Gamma}_3(s_{10}, s_{21}, \eta') = \int \frac{d\omega}{2\pi i} e^{\omega(\eta'-s_{21})} \left[\bar{\Gamma}_{3\omega}^+(s_{10}) e^{\delta_\omega^+ s_{21}} + \bar{\Gamma}_{3\omega}^-(s_{10}) e^{\delta_\omega^- s_{21}} \right] \quad (34c)$$

$$+ \int \frac{d\omega}{2\pi i} \int \frac{d\gamma}{2\pi i} \left\{ e^{\omega(\eta'-s_{10})+\gamma s_{10}} \left[-\vec{V}_{\text{UV}} \cdot \vec{I}_{\omega\gamma}^{(0)} + G_{2\omega\gamma}^{(0)} \right] \right. \\ \left. + e^{\omega(\eta'-s_{21})+\gamma s_{10}} \left[G_{2\omega\gamma} - G_{2\omega\gamma}^{(0)} + \vec{V}_{\text{UV}} \cdot \vec{I}_{\omega\gamma}^{(0)} - \vec{V}_{\text{UV}} \cdot (2\omega\gamma - M_{\text{IR}})^{-1} (2\omega\gamma \vec{I}_{\omega\gamma}^{(0)} + G_{\omega\gamma} \vec{V}_G + G_{2\omega\gamma} \vec{V}_{G_2}) \right] \right\}$$

$$\vec{\Gamma}(s_{10}, s_{21}, \eta') = \int \frac{d\omega}{2\pi i} \int \frac{d\gamma}{2\pi i} \left\{ e^{\omega(\eta'-s_{10})+\gamma s_{10}} \vec{I}_{\omega\gamma}^{(0)} \right. \\ \left. + e^{\omega(\eta'-s_{21})+\gamma s_{10}} \left[(2\omega\gamma - M_{\text{IR}})^{-1} \left(2\omega\gamma \vec{I}_{\omega\gamma}^{(0)} + \vec{V}_G G_{\omega\gamma} + \vec{V}_{G_2} G_{2\omega\gamma} + \vec{V}_{\bar{I}_3} \bar{I}_{3\omega\gamma} \right) - \vec{I}_{\omega\gamma}^{(0)} \right] \right\}, \quad (34d)$$

where

$$f^{(0)}(s_{10}, \eta) = \int \frac{d\omega}{2\pi i} \int \frac{d\gamma}{2\pi i} e^{\omega(\eta-s_{10})+\gamma s_{10}} f_{\omega\gamma}^{(0)}, \quad (35a)$$

$$\bar{I}_{3\omega\gamma} = \frac{\vec{V}_{\text{UV}} \cdot \left(\vec{I}_{\omega\gamma}^{(0)} - \vec{I}_{\delta_\omega^\pm \gamma}^{(0)} \right) - G_{2\omega\gamma}^{(0)} + G_{2\delta_\omega^\pm \gamma}^{(0)} - \vec{I}_{3\delta_\omega^\pm \gamma}^{(0)}}{(\omega\delta_\omega^- - 1) \vec{V}_{\text{UV}} \cdot (2\omega\gamma - M_{\text{IR}})^{-1} \vec{V}_{\bar{I}_3} - 1} \\ + \frac{(\omega\delta_\omega^- - 1) \left[G_{2\omega\gamma} - G_{2\omega\gamma}^{(0)} + \vec{V}_{\text{UV}} \cdot \vec{I}_{\omega\gamma}^{(0)} - \vec{V}_{\text{UV}} \cdot (2\omega\gamma - M_{\text{IR}})^{-1} (2\omega\gamma \vec{I}_{\omega\gamma}^{(0)} + G_{\omega\gamma} \vec{V}_G + G_{2\omega\gamma} \vec{V}_{G_2}) \right]}{(\omega\delta_\omega^- - 1) \vec{V}_{\text{UV}} \cdot (2\omega\gamma - M_{\text{IR}})^{-1} \vec{V}_{\bar{I}_3} - 1}, \quad (35b)$$

$$\bar{\Gamma}_{3\omega}^\pm(s_{10}) = e^{-\delta_\omega^\pm s_{10}} \frac{\delta_\omega^\pm}{\delta_\omega^\pm - \delta_\omega^\mp} \int \frac{d\gamma}{2\pi i} e^{\gamma s_{10}} \left\{ (\omega\delta_\omega^\mp - 1) \left[G_{2\omega\gamma} - G_{2\omega\gamma}^{(0)} - \vec{V}_{\text{UV}} \cdot \left(\vec{I}_{\omega\gamma} - \vec{I}_{\omega\gamma}^{(0)} \right) \right] \right. \\ \left. - G_{2\omega\gamma}^{(0)} + \vec{V}_{\text{UV}} \cdot \vec{I}_{\omega\gamma}^{(0)} + \bar{I}_{3\omega\gamma} \right\}, \quad (35c)$$

$$G_{2\omega\gamma} = G_{2\omega\gamma}^{(0)} + \frac{2(\gamma - \delta_\omega^+) \left(G_{\delta_\omega^+ \gamma}^{(0)} + 2G_{2\delta_\omega^+ \gamma}^{(0)} \right) - 2(\gamma_\omega^+ - \delta_\omega^+) \left(G_{\delta_\omega^+ \gamma_\omega^+}^{(0)} + 2G_{2\delta_\omega^+ \gamma_\omega^+}^{(0)} \right) + 8\delta_\omega^- \left(G_{2\omega\gamma}^{(0)} - G_{2\omega\gamma_\omega^+}^{(0)} \right)}{\omega(\gamma - \gamma_\omega^-)(\gamma - \gamma_\omega^+)}, \quad (35d)$$

$$G_{\omega\gamma} = \frac{1}{2} \omega\gamma (G_{2\omega\gamma} - G_{2\omega\gamma}^{(0)}) - 2G_{2\omega\gamma}, \quad (35e)$$

for $f \in \{G, G_2, \bar{I}_3, \vec{I}\}$, and, as defined above, we have

$$\delta_\omega^\pm \equiv \frac{\omega}{2} \left[1 \pm \sqrt{1 - \frac{4}{\omega^2}} \right], \quad (36a)$$

$$\gamma_\omega^\pm \equiv \frac{\omega}{2} \left[1 \pm \sqrt{1 - \frac{16}{\omega^2} \sqrt{1 - \frac{4}{\omega^2}}} \right], \quad (36b)$$

$$\vec{V}_{\text{UV}} \equiv (-2, -1, 3), \quad (36c)$$

$$\vec{V}_{\bar{I}_3} \equiv (0, -2, 0), \quad (36d)$$

$$\vec{V}_G \equiv (0, 2, 2), \quad (36e)$$

$$\vec{V}_{G_2} \equiv (1, 3, 4), \quad (36f)$$

$$M_{\text{IR}} \equiv \begin{pmatrix} 4 & 2 & -2 \\ 2 & -1 & -3 \\ 0 & 0 & 0 \end{pmatrix}. \quad (36g)$$

With the exact expressions for the polarized dipole and moment amplitudes in hand, we can now write down the helicity PDFs and OAM distributions. Plugging Eqs. (34) with Eq. (35) into Eqs. (20) gives

$$L_{q+\bar{q}}(x, Q^2) = \frac{N_f}{\alpha_s \pi^2} \int \frac{d\omega}{2\pi i} \int \frac{d\gamma}{2\pi i} \frac{e^{\sqrt{\alpha_s} \omega \ln(1/x) + \sqrt{\alpha_s} \gamma \ln(Q^2/\Lambda^2)}}{\gamma(\omega - \gamma)} \left[G_{\omega\gamma} - 3 G_{2\omega\gamma} - \bar{I}_{3\omega\gamma} \right. \\ \left. + (\vec{V}_{\text{UV}} - 2 \vec{V}_{\bar{I}_3}) \cdot (2\omega\gamma - M_{\text{IR}})^{-1} \left(2\omega\gamma \vec{I}_{\omega\gamma}^{(0)} + G_{\omega\gamma} \vec{V}_G + G_{2\omega\gamma} \vec{V}_{G_2} + \vec{V}_{\bar{I}_3} \bar{I}_{3\omega\gamma} \right) \right], \quad (37a)$$

$$L_G(x, Q^2) = -\frac{2N_c}{\alpha_s \pi^2} \int \frac{d\omega}{2\pi i} \int \frac{d\gamma}{2\pi i} e^{\sqrt{\alpha_s} \omega \ln(1/x) + \sqrt{\alpha_s} \gamma \ln(Q^2/\Lambda^2)} \\ \times \left(2 \vec{V}_G - \vec{V}_{\text{UV}} + \vec{V}_{\bar{I}_3} \right) \cdot (2\omega\gamma - M_{\text{IR}})^{-1} \left(2\omega\gamma \vec{I}_{\omega\gamma}^{(0)} + G_{\omega\gamma} \vec{V}_G + G_{2\omega\gamma} \vec{V}_{G_2} + \vec{V}_{\bar{I}_3} \bar{I}_{3\omega\gamma} \right), \quad (37b)$$

$$\Delta\Sigma(x, Q^2) = -\frac{N_f}{\alpha_s \pi^2} \int \frac{d\omega}{2\pi i} \int \frac{d\gamma}{2\pi i} \frac{e^{\sqrt{\alpha_s} \omega \ln(1/x) + \sqrt{\alpha_s} \gamma \ln(Q^2/\Lambda^2)}}{\gamma(\omega - \gamma)} \left[G_{\omega\gamma} + 2 G_{2\omega\gamma} \right], \quad (37c)$$

$$\Delta G(x, Q^2) = \frac{2N_c}{\alpha_s \pi^2} \int \frac{d\omega}{2\pi i} \int \frac{d\gamma}{2\pi i} e^{\sqrt{\alpha_s} \omega \ln(1/x) + \sqrt{\alpha_s} \gamma \ln(Q^2/\Lambda^2)} G_{2\omega\gamma}, \quad (37d)$$

where, as above in Eqs. (20), we have defined $\bar{\alpha}_s \equiv \frac{\alpha_s N_c}{2\pi}$. In arriving at Eqs. (37a) and (37c), we have done the s_{10} and η integrals in Eqs. (20a) and (20c). We emphasize here that, while Eqs. (37a) and (37b) were derived in [1], here we have explicitly found the double Laplace images. As mentioned above, Eqs. (37c) and (37d) were derived in [59] and the double Laplace images were found in [3].

All together, Eqs. (37) give the exact small- x , large- N_c DLA expressions for the quark and gluon OAM distributions and the quark and gluon helicity PDFs.

B. Small- x asymptotics of the OAM distributions

From Eqs. (37a) and (37b), we can see that the small- x asymptotics of the OAM distributions are governed by the rightmost singularity in the ω -plane. One can show this singularity is given by setting the large square root in γ_{ω}^{-} to 0 [3], which gives

$$1 - \frac{16}{\omega^2} \sqrt{1 - \frac{4}{\omega^2}} = 0. \quad (38)$$

The solution to Eq. (38) with the largest real part is [3]

$$\omega_b \equiv \frac{4}{3^{1/3}} \sqrt{\text{Re} \left[\left(-9 + i\sqrt{111} \right)^{1/3} \right]} \approx 3.66074. \quad (39)$$

Via Eqs. (37a) and (37b), the small- x asymptotics of the quark and gluon OAM distributions are then

$$L_{q+\bar{q}}(x, Q^2) \sim L_G(x, Q^2) \sim \left(\frac{1}{x} \right)^{\omega_b \sqrt{\frac{\alpha_s N_c}{2\pi}}}. \quad (40)$$

Eq. (40), along with the solution of the small- x , large- N_c evolution equations for the moment amplitudes, Eqs. (34), represent the main result of this work.

Importantly, the OAM distributions have the same intercept $\alpha_h \equiv \omega_b \sqrt{\frac{\alpha_s N_c}{2\pi}}$ as the helicity PDFs. In fact, one can explicitly remove (by hand) the mixing with G, G_2 , and Γ_2 and solve Eqs. (14). The resulting solution has small- x asymptotics that are also governed by the rightmost singularity in the ω -plane. In this case however, one finds the rightmost singularity to be $\omega'_b = 2 < \omega_b$. This is similar to the study of the OAM distributions based on the KPS equations in [2]. There, the “moment amplitudes” were sub-leading at small- x and did not mix with G, G_2 , or Γ_2 under evolution.

Therefore, one can trace the leading small- x , large- N_c asymptotic behavior of the OAM distributions to the mixing of the moment amplitudes with the helicity amplitudes G , G_2 , and Γ_2 under evolution.² This situation is similar to the polarized DGLAP evolution equations for the OAM distributions in the Wandzura-Wilczek approximation [17, 36]. There, the (twist-2 part of the) OAM distributions mix with the helicity PDFs. The leading asymptotic behavior of the (twist-2 part of the) OAM distributions is given by the anomalous dimensions of the helicity PDFs. As we do not employ the Wandzura-Wilczek approximation in this work, it appears the inclusion of genuine twist-3 terms, at least in the case of the small- x evolution presented here, does not affect this conclusion.

We should compare the result in Eq. (40) to the one obtained in [4]. In [4], the BER IREE formalism was extended to the OAM distributions. The resulting OAM distributions were found to obey the same small- x asymptotics as the helicity PDFs. Namely, they found (see Eq. (7) of [4])

$$L_{q+\bar{q}}(x, Q^2) \sim L_G(x, Q^2) \sim \left(\frac{1}{x}\right)^{\alpha_h^{BER}}, \quad (41)$$

where α_h^{BER} is the intercept of both the quark and gluon helicity PDFs. The analytic expression for α_h^{BER} in the large- N_c limit, given in [49] and for which the detailed solution is given in [3], is

$$\alpha_h^{BER} \equiv \sqrt{\frac{17 + \sqrt{97}}{2}} \sqrt{\frac{\alpha_s N_c}{2\pi}} \approx 3.66394 \sqrt{\frac{\alpha_s N_c}{2\pi}}. \quad (42)$$

Comparing Eqs. (40) and (41), we see a slight difference between the intercepts of the OAM distributions found above in the LCOT formalism and found in [4] using the BER IREE formalism. This small discrepancy is the same as the one between the helicity PDF intercepts obtained in the LCOT formalism [3, 59] and the intercepts obtained by BER [39, 40]. See the Appendix of [3] for an explanation of the potential origin of this discrepancy.

V. OAM TO HELICITY PDF RATIOS

Now that we have the analytic expressions for the quark and gluon OAM distributions at small- x and large- N_c , we can explicitly calculate the ratio of the OAM distributions to the helicity PDFs. These ratios have previously been studied in [1, 2, 4, 48, 77, 78], with a discrepancy in the quark ratio between [4] and the numerical solution of [1]. We seek here to investigate this claim and reveal any insight that can be obtained from the exact solution of the moment amplitude evolution.

To start, we evaluate Eqs. (37) for specific initial conditions. Then we take the ratio of Eq. (37a) to Eq. (37c) and Eq. (37b) to Eq. (37d) to obtain the quark and gluon ratios respectively. In [1], it was found the asymptotic ($x \rightarrow 0$) behavior of these ratios is independent of the initial conditions of both the helicity and moment evolution. Therefore, without loss of generality, we choose the following initial conditions

$$G^{(0)}(s_{10}, \eta) = 1, \quad (43a)$$

$$\bar{I}_3^{(0)}(s_{10}, \eta) = \bar{I}^{(0)}(s_{10}, \eta) = G_2^{(0)}(s_{10}, \eta) = 0. \quad (43b)$$

Using Eqs. (43) in Eqs. (35) gives

$$G_{\omega\gamma}^{(0)} = \frac{1}{\omega\gamma}, \quad (44a)$$

$$\bar{I}_{3\omega\gamma}^{(0)} = \bar{I}_{\omega\gamma}^{(0)} = G_{2\omega\gamma}^{(0)} = 0, \quad (44b)$$

$$G_{\omega\gamma} = \frac{\gamma_{\omega}^{-}(\omega\gamma - 4)}{4\gamma(\gamma - \gamma_{\omega}^{-})(2\delta_{\omega}^{+} - \omega)}, \quad (44c)$$

$$G_{2\omega\gamma} = \frac{\gamma_{\omega}^{-}}{2\gamma(\gamma - \gamma_{\omega}^{-})(2\delta_{\omega}^{+} - \omega)}, \quad (44d)$$

$$\bar{I}_{3\omega\gamma} = \frac{\gamma_{\omega}^{-}(2 - \gamma\omega)(\delta_{\omega}^{-}\omega - 1)}{4\gamma\omega^2(\gamma - \gamma_{\omega}^{-})(2\delta_{\omega}^{+} - \omega)(\gamma - \bar{\gamma}_{\omega}^{-})(\gamma - \bar{\gamma}_{\omega}^{+})}, \quad (44e)$$

² Note that $G(s_{10}, \eta)$ and $G_2(s_{10}, \eta)$ also explicitly appear in the expression for the quark OAM distribution, Eq. (20a).

where we have defined

$$2\gamma^2\omega^2 - \gamma\omega(5 + 2\delta_\omega^-\omega) + 4 \equiv 2\omega^2(\gamma - \bar{\gamma}_\omega^+)(\gamma - \bar{\gamma}_\omega^-). \quad (45)$$

Now, using Eqs. (44) in Eqs. (37) gives

$$L_{q+\bar{q}}(y, t) = \frac{N_f}{\alpha_s\pi^2} \int \frac{d\omega}{2\pi i} \int \frac{d\gamma}{2\pi i} e^{\omega y + \gamma t} \frac{\gamma_\omega^- \omega \left[2\gamma^3\omega^2 - \gamma^2\omega(13 + 2\delta_\omega^-\omega) + 2\gamma(6 + 5\delta_\omega^-\omega) + 12\delta_\omega^- \right]}{4\gamma^2(\gamma - \gamma_\omega^-)(\gamma - \omega)(\omega - 2\delta_\omega^+)(\gamma - \bar{\gamma}_\omega^+)(\gamma - \bar{\gamma}_\omega^-)}, \quad (46a)$$

$$L_G(y, t) = -\frac{2N_c}{\alpha_s\pi^2} \int \frac{d\omega}{2\pi i} \int \frac{d\gamma}{2\pi i} e^{\omega y + \gamma t} \frac{\gamma_\omega^- \left[4\gamma^2\omega^2 - \gamma\omega(11 + 4\delta_\omega^-\omega) + 4\delta_\omega^-\omega + 8 \right]}{2\gamma(\gamma - \gamma_\omega^-)(2\delta_\omega^+ - \omega)(\gamma - \bar{\gamma}_\omega^+)(\gamma - \bar{\gamma}_\omega^-)}, \quad (46b)$$

$$\Delta\Sigma(y, t) = -\frac{N_f}{\alpha_s\pi^2} \int \frac{d\omega}{2\pi i} \int \frac{d\gamma}{2\pi i} e^{\omega y + \gamma t} \frac{\gamma_\omega^- \omega}{4\gamma(\gamma - \gamma_\omega^-)(\gamma - \omega)(\omega - 2\delta_\omega^+)}, \quad (46c)$$

$$\Delta G(y, t) = \frac{2N_c}{\alpha_s\pi^2} \int \frac{d\omega}{2\pi i} \int \frac{d\gamma}{2\pi i} e^{\omega y + \gamma t} \frac{\gamma_\omega^-}{2\gamma(\gamma - \gamma_\omega^-)(2\delta_\omega^+ - \omega)}, \quad (46d)$$

where we have expressed both the OAM distributions and hPDFs with the arguments $y = \sqrt{\alpha_s} \ln 1/x$ and $t = \sqrt{\alpha_s} \ln Q^2/\Lambda^2$. We will use these arguments for the rest of this Section, since such variables appear more natural in our expressions as can be seen from Eqs. (37). Now we close the γ -contours in Eqs. (46) to the left. (Note that $\text{Re } \omega > \text{Re } \gamma$ along the integration contours.) The result is

$$L_{q+\bar{q}}(y, t) = \frac{N_f}{\alpha_s\pi^2} \int \frac{d\omega}{2\pi i} \frac{e^{\omega y}}{8\gamma_\omega^- \omega^3 (\omega - 2\delta_\omega^+)} \left\{ \frac{10\bar{\gamma}_\omega^- \bar{\gamma}_\omega^+ \gamma_\omega^- \delta_\omega^- \omega^2}{(\bar{\gamma}_\omega^-)^2 (\bar{\gamma}_\omega^+)^2} \right. \quad (47a)$$

$$+ \frac{12\bar{\gamma}_\omega^- \bar{\gamma}_\omega^+ \gamma_\omega^- \delta_\omega^- + 12\omega \bar{\gamma}_\omega^- \bar{\gamma}_\omega^+ \gamma_\omega^- + 12\omega \bar{\gamma}_\omega^+ \gamma_\omega^- \delta_\omega^- + 12\omega \bar{\gamma}_\omega^+ \delta_\omega^- (\bar{\gamma}_\omega^+ + \gamma_\omega^- + t\bar{\gamma}_\omega^+ \gamma_\omega^-)}{(\bar{\gamma}_\omega^-)^2 (\bar{\gamma}_\omega^+)^2}$$

$$+ e^{\bar{\gamma}_\omega^- t} \frac{(\gamma_\omega^-)^2 \omega^2 (12\delta_\omega^- + 12\bar{\gamma}_\omega^- + \omega \bar{\gamma}_\omega^- [10\delta_\omega^- - 13\bar{\gamma}_\omega^- + 2\bar{\gamma}_\omega^- \omega (\bar{\gamma}_\omega^- - \delta_\omega^-)])}{(\bar{\gamma}_\omega^-)^2 (\bar{\gamma}_\omega^- - \bar{\gamma}_\omega^+) (\bar{\gamma}_\omega^- - \gamma_\omega^-) (\bar{\gamma}_\omega^- - \omega)}$$

$$+ e^{\bar{\gamma}_\omega^+ t} \frac{(\gamma_\omega^-)^2 \omega^2 (12\delta_\omega^- + 12\bar{\gamma}_\omega^+ + \omega \bar{\gamma}_\omega^+ [10\delta_\omega^- - 13\bar{\gamma}_\omega^+ + 2\bar{\gamma}_\omega^+ \omega (\bar{\gamma}_\omega^+ - \delta_\omega^-)])}{(\bar{\gamma}_\omega^+)^2 (\bar{\gamma}_\omega^+ - \bar{\gamma}_\omega^-) (\bar{\gamma}_\omega^+ - \gamma_\omega^-) (\bar{\gamma}_\omega^+ - \omega)}$$

$$+ e^{\gamma_\omega^- t} \frac{\omega^2 (12\delta_\omega^- + 12\bar{\gamma}_\omega^- + \omega \bar{\gamma}_\omega^- [10\delta_\omega^- - 13\bar{\gamma}_\omega^- + 2\bar{\gamma}_\omega^- \omega (\bar{\gamma}_\omega^- - \delta_\omega^-)])}{(\bar{\gamma}_\omega^- - \bar{\gamma}_\omega^-) (\bar{\gamma}_\omega^- - \bar{\gamma}_\omega^+) (\bar{\gamma}_\omega^- - \omega)} \Big\},$$

$$L_G(y, t) = -\frac{2N_c}{\alpha_s\pi^2} \int \frac{d\omega}{2\pi i} \frac{e^{\omega y} \gamma_\omega^-}{2(2\delta_\omega^+ - \omega)} \left[e^{\gamma_\omega^- t} \frac{4(\gamma_\omega^-)^2 \omega^2 - \gamma_\omega^- \omega (11 + 4\delta_\omega^-\omega) + 4\delta_\omega^-\omega + 8}{2\bar{\gamma}_\omega^- (\bar{\gamma}_\omega^- - \bar{\gamma}_\omega^+) (\bar{\gamma}_\omega^- - \bar{\gamma}_\omega^-)} - \frac{4\delta_\omega^-\omega + 8}{2\bar{\gamma}_\omega^- \bar{\gamma}_\omega^+ \bar{\gamma}_\omega^-} \right. \quad (47b)$$

$$+ e^{\bar{\gamma}_\omega^+ t} \frac{4(\bar{\gamma}_\omega^+)^2 \omega^2 - \bar{\gamma}_\omega^+ \omega (11 + 4\delta_\omega^-\omega) + 4\delta_\omega^-\omega + 8}{2\bar{\gamma}_\omega^+ (\bar{\gamma}_\omega^+ - \gamma_\omega^-) (\bar{\gamma}_\omega^+ - \bar{\gamma}_\omega^-)} + e^{\bar{\gamma}_\omega^- t} \frac{4(\bar{\gamma}_\omega^-)^2 \omega^2 - \bar{\gamma}_\omega^- \omega (11 + 4\delta_\omega^-\omega) + 4\delta_\omega^-\omega + 8}{2\bar{\gamma}_\omega^- (\bar{\gamma}_\omega^- - \gamma_\omega^-) (\bar{\gamma}_\omega^- - \bar{\gamma}_\omega^+)} \Big],$$

$$\Delta\Sigma(y, t) = -\frac{N_f}{\alpha_s\pi^2} \int \frac{d\omega}{2\pi i} \frac{e^{\omega y} \omega}{4(\omega - 2\delta_\omega^+)} \left[\frac{1}{\omega} + \frac{e^{\gamma_\omega^- t}}{\gamma_\omega^- - \omega} \right], \quad (47c)$$

$$\Delta G(y, t) = \frac{2N_c}{\alpha_s\pi^2} \int \frac{d\omega}{2\pi i} \frac{e^{\omega y}}{2(\delta_\omega^+ - \omega)} \left[e^{\gamma_\omega^- t} - 1 \right]. \quad (47d)$$

Due to the complex branch structure of the integrands in Eqs. (47), we approximate the ω -integrals. Since we would like to determine the OAM to hPDF ratios in the asymptotic limit, where there is little to no dependence on the initial conditions, it suffices to evaluate the integrals in Eqs. (47) to leading order in y only. The leading order behavior is given by the rightmost singularity in the ω -plane, as mentioned above. Some of the branch structure beyond this rightmost singularity is shown in Fig. 6 of [1]. There is a branch cut along the real axis from ω_b to some ω'_b where $\omega'_b < \omega_b$. Therefore, to evaluate any one of the integrals in Eqs. (47), one can wrap the contour across this branch cut and approximate the integrals as the integrals of the discontinuity across the branch cut. If we label the integrands (including pre-factors) of Eqs. (47) via $L_{q+\bar{q},\omega}$, $L_{G,\omega}$, $\Delta\Sigma_\omega$, and ΔG_ω , we may write this approximation as

$$L_{q+\bar{q}}(y, t) \approx \lim_{\epsilon \rightarrow 0^+} \int_0^\infty \frac{d\xi}{2\pi i} (L_{q+\bar{q},\omega_b - \xi + i\epsilon} - L_{q+\bar{q},\omega_b - \xi - i\epsilon}), \quad (48a)$$

$$L_G(y, t) \approx \lim_{\epsilon \rightarrow 0^+} \int_0^\infty \frac{d\xi}{2\pi i} (L_{G, \omega_b - \xi + i\epsilon} - L_{G, \omega_b - \xi - i\epsilon}), \quad (48b)$$

$$\Delta\Sigma(y, t) \approx \lim_{\epsilon \rightarrow 0^+} \int_0^\infty \frac{d\xi}{2\pi i} (\Delta\Sigma_{\omega_b - \xi + i\epsilon} - \Delta\Sigma_{\omega_b - \xi - i\epsilon}), \quad (48c)$$

$$\Delta G(y, t) \approx \lim_{\epsilon \rightarrow 0^+} \int_0^\infty \frac{d\xi}{2\pi i} (\Delta G_{\omega_b - \xi + i\epsilon} - \Delta G_{\omega_b - \xi - i\epsilon}), \quad (48d)$$

where, due to the y -dependent exponentials in Eqs. (47), we have extended the ξ -integration to infinity, and discarded the rest of the contribution from closing the contour as subleading. One can also think of this as sending $\omega'_b \rightarrow -\infty$. Now it is a simple matter to plug Eqs. (47) into Eqs. (48) and compute the integrals. However, since we are only interested in the leading order (in y) result, one can expand the integrands (excluding the large exponentials $e^{-\xi y}$) around $\xi = 0$, and keep only the leading terms. The resulting integral is then a power series in $1/y$ multiplied by the leading exponential. For example, this series is explicitly constructed for Eqs. (48c) and (48d) in the Appendix of [1]. When one takes the ratio of Eq. (48a) to Eq. (48c) or Eq. (48b) to Eq. (48d), the result is again a series in $1/y$. We can then write the ratios of Eq. (48a) to Eq. (48c) and Eq. (48b) to Eq. (48d) as

$$\frac{L_{q+\bar{q}}(y, t)}{\Delta\Sigma(y, t)} = R_q(t) + \frac{B_q(t)}{y} + \mathcal{O}\left(\frac{1}{y^2}\right), \quad (49a)$$

$$\frac{L_G(y, t)}{\Delta G(y, t)} = R_G(t) + \frac{B_G(t)}{y} + \mathcal{O}\left(\frac{1}{y^2}\right). \quad (49b)$$

The explicit expressions for the asymptotic ratios, $R_q(t)$ and $R_G(t)$, are given in Appendix C. In Fig. 1, we show $R_q(t)$, $B_q(t)$, $R_G(t)$, and $B_G(t)$ for the branch cut discontinuity approximation in Eqs. (48) as a function of t . In Fig. 1, we plot $R_q(t)$, $B_q(t)$, $R_G(t)$, $B_G(t)$ in panels (a), (b), (c), and (d) respectively. Additionally, we give the explicit values of $R_q(t)$, $B_q(t)$, $R_G(t)$, and $B_G(t)$ for some values of t in Table I.

t	$R_q(t)$	$B_q(t)$	$R_G(t)$	$B_G(t)$
0.1	-0.668	0.296	-1.994	0.002
0.5	-0.616	0.358	-1.975	0.013
1.0	-0.549	0.491	-1.962	0.024
1.5	-0.498	0.649	-1.956	0.034

TABLE I: Specific values of the coefficients $R_q(t)$, $B_q(t)$, $R_G(t)$, $B_G(t)$ in Eqs. (49) for various values of $t = \sqrt{\alpha_s} \ln Q^2/\Lambda^2$. Here $N_c = 3$ and $\alpha_s = 0.25$.

We should compare the results in Fig. 1 and Table I to the predictions from [4]. From Eqs. (6) and (7) in [4], after using the fact that the parameter $\alpha \sim \sqrt{\alpha_s}$ is perturbatively small, we see, in the DLA, [4] predicts

$$\frac{L_{q+\bar{q}}(y, t)}{\Delta\Sigma(y, t)} = -1, \quad (50a)$$

$$\frac{L_G(y, t)}{\Delta G(y, t)} = -2. \quad (50b)$$

Comparing these results to Fig. 1 and Table I, we see that we predict nearly the same value for the asymptotic gluon ratio, $R_G(t)$. In the quark sector, our $R_q(t)$ is nearly half that of [4]. In both the quark and gluon sectors, we note from Fig. 1, our results are dependent on $t = \sqrt{\alpha_s} \ln Q^2/\Lambda^2$, and as t increases, the asymptotic ratios, $R_q(t)$ and $R_G(t)$, get further away from the results of [4]. Therefore, we conclude that both the quark and gluon ratios determined here disagree with the results of [4]. This is contrast to [1], where the numerically small difference in the gluon sector could have been attributed to underestimation of the numerical error.

The ratios in Fig. 1 are consistent with the numerical findings of [1]. Among the potential sources of the discrepancy between the quark ratio of [4] and ours in Fig. 1 and Table I is the implementation of the large- N_c limit. See the discussion below Eq. (71b) of [1] for details. As mentioned there, one could hope that taking the large- N_c & N_f limit, as done in [59], might account for the discrepancy. However, as mentioned in [1], a preliminary numerical solution of the large- N_c & N_f moment amplitude evolution equations for $N_f/N_c \rightarrow 0$ has been constructed and has not been able to account for the discrepancy in the quark ratio. A full analysis of the large- N_c & N_f limit is left for future work. Additionally, the Wandzura-Wilczek approximation [79], which neglects the genuine twist-3 contributions to

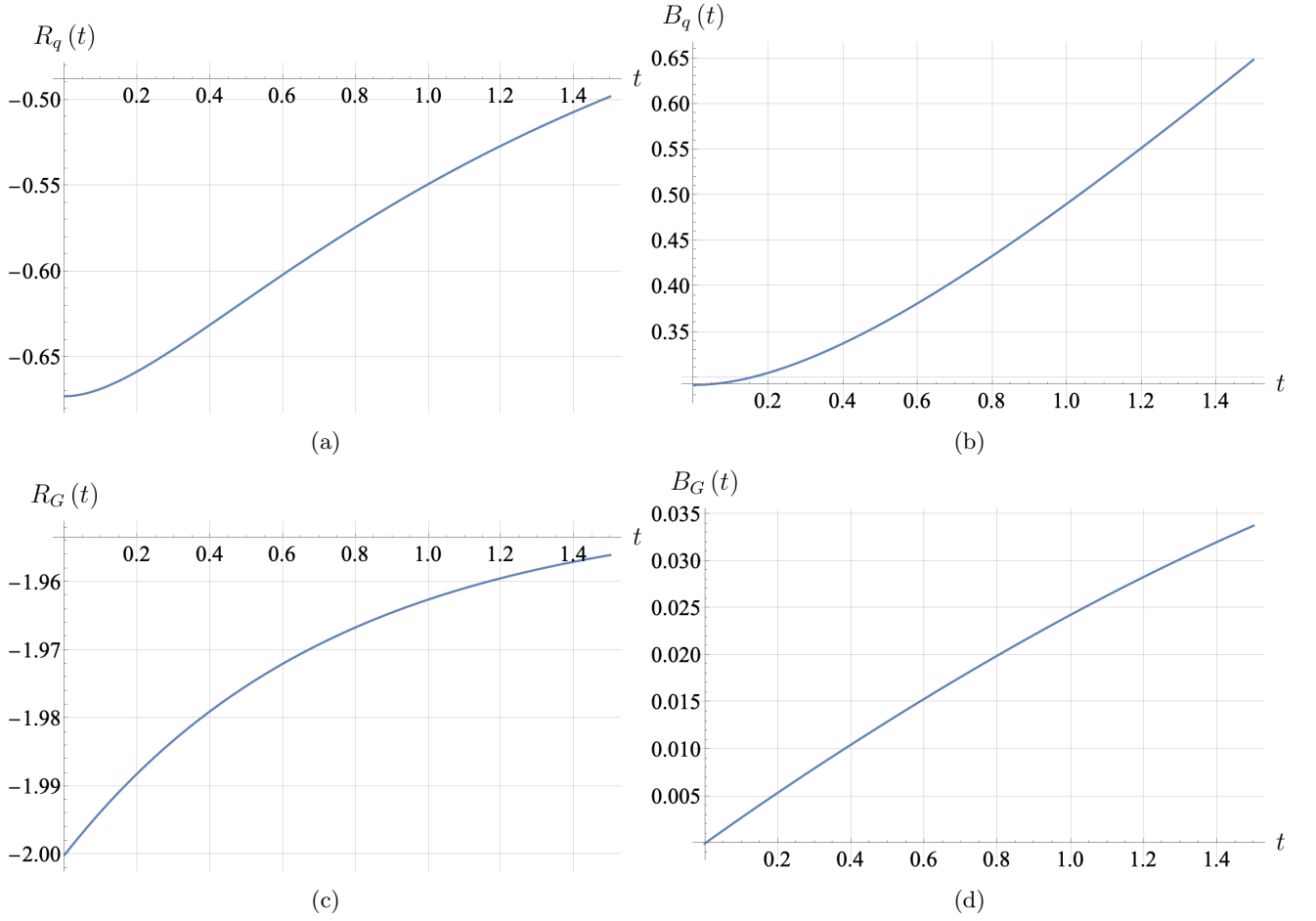


FIG. 1: Plots of the coefficients $R_q(t)$, $B_q(t)$, $R_G(t)$, $B_G(t)$ from Eqs. (49) as a function of t resulting from the branch cut discontinuity approximation in Eqs. (48). Here $N_c = 3$ and $\alpha_s = 0.25$.

the OAM distributions, is employed in [4]. Although the twist-3 contributions, particularly their evolution in Q^2 , have been studied in [80], a dedicated small- x study has not yet been performed. So far in this work, we have not identified the twist-3 contribution to the OAM distributions explicitly. To examine their effect on the OAM to hPDF ratios, let us attempt to isolate the twist-3 contributions explicitly.

We start with the following relations derived in [19],

$$L_{q+\bar{q}}(x, Q^2) = x \int_x^1 \frac{dx'}{x'} \left[H_q(x', Q^2) + E_q(x', Q^2) \right] - x \int_x^1 \frac{dx'}{x'^2} \Delta \Sigma(x', Q^2) + L_{q+\bar{q}}^3(x, Q^2), \quad (51a)$$

$$L_G(x, Q^2) = x \int_x^1 \frac{dx'}{x'} \left[H_g(x', Q^2) + E_g(x', Q^2) \right] - 2x \int_x^1 \frac{dx'}{x'^2} \Delta G(x', Q^2) + L_G^3(x, Q^2), \quad (51b)$$

where $H_{q(g)}(x, Q^2)$, $E_{q(g)}(x, Q^2)$ are the standard unpolarized quark (gluon) twist-2 generalized parton distributions (GPDs) at zero skewness and in the limit of zero momentum transfer. $L_{q+\bar{q}}^3(x, Q^2)$ and $L_G^3(x, Q^2)$ are the twist-3 contributions to the quark and gluon OAM distributions respectively. They can be expressed using twist-3 GPDs [19], and they are the neglected contributions in the Wandzura-Wilczek approximation. Since we are working in the DLA, we can neglect the unpolarized twist-2 GPDs, as their evolution is single-logarithmic.

Then, via Eqs. (51), we can write the DLA expressions for the twist-3 contributions to the quark and gluon OAM distributions as

$$L_{q+\bar{q}}^3(x, Q^2) = L_{q+\bar{q}}(x, Q^2) + x \int_x^1 \frac{dx'}{x'^2} \Delta \Sigma(x', Q^2), \quad (52a)$$

$$L_G^3(x, Q^2) = L_G(x, Q^2) + 2x \int_x^1 \frac{dx'}{x'^2} \Delta G(x', Q^2). \quad (52b)$$

Similarly, we write the DLA twist-2, Wandzura-Wilczek (WW) contribution to the OAM distributions as [4, 19]

$$L_{q+\bar{q}}^{WW}(x, Q^2) = -x \int_x^1 \frac{dx'}{x'^2} \Delta \Sigma(x', Q^2), \quad (53a)$$

$$L_G^{WW}(x, Q^2) = -2x \int_x^1 \frac{dx'}{x'^2} \Delta G(x', Q^2). \quad (53b)$$

Then, using Eqs. (52) and (53), we may write the asymptotic limit of Eqs. (49) as

$$\lim_{y \rightarrow \infty} \frac{L_{q+\bar{q}}(y, t)}{\Delta \Sigma(y, t)} = \lim_{y \rightarrow \infty} \frac{L_{q+\bar{q}}^{WW}(y, t)}{\Delta \Sigma(y, t)} + \lim_{y \rightarrow \infty} \frac{L_{q+\bar{q}}^3(y, t)}{\Delta \Sigma(y, t)} \equiv R_q^{WW}(t) + R_q^3(t), \quad (54a)$$

$$\lim_{y \rightarrow \infty} \frac{L_G(y, t)}{\Delta G(y, t)} = \lim_{y \rightarrow \infty} \frac{L_G^{WW}(y, t)}{\Delta G(y, t)} + \lim_{y \rightarrow \infty} \frac{L_G^3(y, t)}{\Delta G(y, t)} \equiv R_G^{WW}(t) + R_G^3(t), \quad (54b)$$

where we have again used the more convenient variables $y = \sqrt{\alpha_s} \ln(1/x)$, $t = \sqrt{\alpha_s} \ln(Q^2/\Lambda^2)$ in the arguments of the OAM distributions and the hPDFs.

As first observed in [4], using the asymptotic form for helicity PDFs and the OAM distributions in Eqs. (53) gives

$$R_q^{WW}(t) = -\frac{1}{1 + \alpha_h}, \quad (55a)$$

$$R_G^{WW}(t) = -\frac{2}{1 + \alpha_h}, \quad (55b)$$

where $\alpha_h = \omega_b \sqrt{\alpha_s}$ for ω_b given above in Eq. (39). To compute the twist-3 part of the ratios in Eqs. (54), we substitute the exact expressions for the OAM distributions and the helicity PDFs from Eqs. (37) into Eqs. (52). We then perform the procedure described above to extract the OAM to hPDF ratios separately for the twist-2 (WW) and twist-3 OAM contributions. The results for the asymptotic ratios for the quark and gluon sector are shown in Fig. 2. As expected, the twist-2 contributions are exactly the values given in Eqs. (55).³ We see from Fig. 2 that the twist-3 contributions vary with t and are similar in magnitude to the twist-2 contributions. Therefore, according to the indirect analysis performed here, it seems as though the twist-3 contributions may be the source of the discrepancy between the OAM to hPDF ratios computed here and those computed in [4].

VI. CONCLUSIONS AND OUTLOOK

Let us summarize what we have accomplished here. We have found an exact solution of the large- N_c equations for the small- x moment amplitude evolution derived in [1], given in Eqs. (8) and (9). This solution is given in Eqs. (34) and (35). With our solution, we have written down expressions for the quark and gluon OAM distributions at large- N_c and small- x , given in Eqs. (37a) and (37b) respectively. We have determined the small- x asymptotics of the quark and gluon OAM distributions in Eq. (40). Notably, we find the small- x behavior is largely driven by the mixing of the moment amplitudes I_3, I_4, I_5, I_6 with the dipole amplitudes G, G_2 , and neighbor amplitude Γ_2 . Therefore, we find the discrepancy for the intercepts of the OAM distributions obtained here and the intercept obtained in [4] to be the same as the discrepancy between the helicity PDF intercepts obtained in the LCOT formalism [3] and the BER formalism [39, 40].

We have also studied the ratios of the quark and gluon OAM distributions to their helicity PDF counterparts in the small- x region. In [1], the quark and gluon ratios in the WW approximation from Eqs. (55) were approximated by $R_q^{WW} \approx -1$ and $R_G^{WW} \approx -2$, with the numerical results of [1] indicating a disagreement of the net quark ratio $R_q = R_q^{WW} + R_q^3$ and R_q^{WW} as well as an agreement between the net ratio gluon ratio $R_G = R_G^{WW} + R_G^3$ and R_G^{WW} within the accuracy of the numerical approximation. We have confirmed these results in addition to finding a small

³ Note that we compute $R_{q/G}^{WW}$ by substituting the full DLA expressions for the helicity PDFs into Eqs. (53), not only the asymptotic forms.

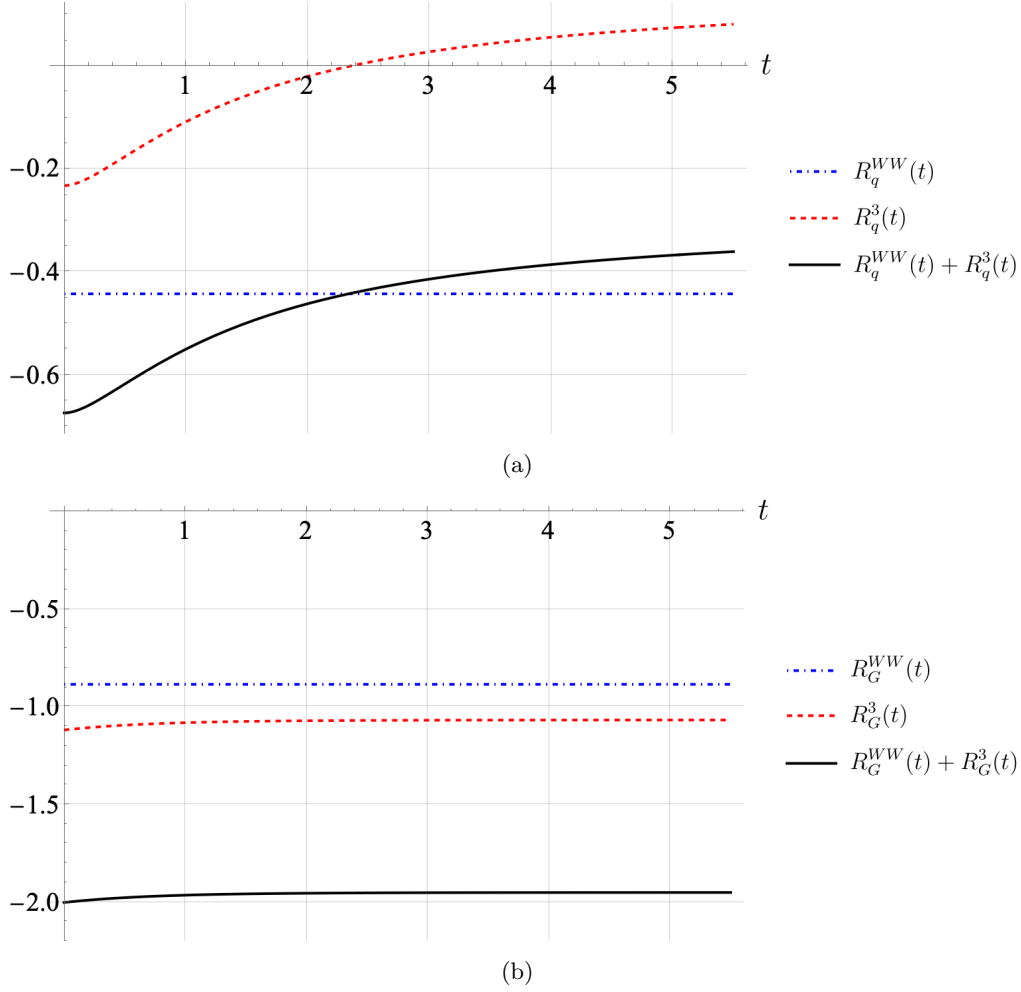


FIG. 2: Plots of the asymptotic ($x \rightarrow 0$) OAM to hPDF ratios for the twist-2 ($R^{WW}(t)$), twist-3 ($R^3(t)$) and full ($R^{WW}(t) + R^3(t)$) OAM distribution contributions in the (a) quark and (b) gluon sector as a function of $t = \sqrt{\alpha_s} \ln(Q^2/\Lambda^2)$. Here $N_c = 3$ and $\alpha_s = 0.25$.

but non-zero disagreement between R_G and $R_G^{WW} \approx -2$. Furthermore, we have found a disagreement between R_q and the full R_q^{WW} given in Eqs. (55), as well as a more significant disagreement between R_G and the full R_G^{WW} . We have tentatively traced these discrepancies to the twist-3 contributions to the OAM distributions. However, a more complete study is warranted to verify this conclusion.

ACKNOWLEDGMENTS

The author would like to thank Yuri Kovchegov, Jeremy Borden and Yoshitaka Hatta for extensive advice and helpful discussions.

This material is based upon work supported by the U.S. Department of Energy, Office of Science, Office of Nuclear Physics under Award Number DE-SC0004286 and is performed within the framework of the Saturated Glue (SURGE) Topical Theory Collaboration.

Appendix A: Boundary conditions

From Eqs. (14) we see there are several boundary conditions that need to be satisfied. From Eqs. (14b) and (14d), we need

$$\vec{I}(s_{10} = 0, \eta) = \vec{I}^{(0)}(s_{10} = 0, \eta), \quad (\text{A1a})$$

$$\vec{I}(s_{10}, \eta = s_{10}) = \vec{I}^{(0)}(s_{10}, \eta = s_{10}), \quad (\text{A1b})$$

$$\vec{\Gamma}(s_{10} = 0, s_{21}, \eta') = \vec{I}^{(0)}(s_{10} = 0, \eta'), \quad (\text{A1c})$$

$$\vec{\Gamma}(s_{10}, s_{21}, \eta' = s_{21}) = \vec{I}^{(0)}(s_{10}, \eta' = s_{21}). \quad (\text{A1d})$$

Plugging in Eqs. (21), we get

$$\int \frac{d\omega}{2\pi i} \int \frac{d\gamma}{2\pi i} e^{\omega\eta} \vec{I}_{\omega\gamma} = \int \frac{d\omega}{2\pi i} \int \frac{d\gamma}{2\pi i} e^{\omega\eta} \vec{I}_{\omega\gamma}^{(0)}, \quad (\text{A2a})$$

$$\int \frac{d\omega}{2\pi i} \int \frac{d\gamma}{2\pi i} e^{\gamma s_{10}} \vec{I}_{\omega\gamma} = \int \frac{d\omega}{2\pi i} \int \frac{d\gamma}{2\pi i} e^{\gamma s_{10}} \vec{I}_{\omega\gamma}^{(0)}. \quad (\text{A2b})$$

Note Eqs. (A1c) and (A1d) are equivalent to Eqs. (A2). Using the fact that $\vec{I}_{3\omega\gamma}, \vec{I}_{\omega\gamma}, G_{\omega\gamma}, G_{2\omega\gamma} \rightarrow 0$ as $\omega \rightarrow \infty$ or $\gamma \rightarrow \infty$ in order for the double Laplace transforms to exist, we see that

$$\int \frac{d\omega}{2\pi i} \frac{1}{\omega\gamma} \left[\vec{I}_{3\omega\gamma} \vec{V}_{\vec{I}_3} + G_{\omega\gamma} \vec{V}_G + G_{2\omega\gamma} \vec{V}_{G_2} + M_{\text{IR}} \vec{I}_{\omega\gamma} \right] = \int \frac{d\gamma}{2\pi i} \frac{1}{\omega\gamma} \left[\vec{I}_{3\omega\gamma} \vec{V}_{\vec{I}_3} + G_{\omega\gamma} \vec{V}_G + G_{2\omega\gamma} \vec{V}_{G_2} + M_{\text{IR}} \vec{I}_{\omega\gamma} \right] = \vec{0}, \quad (\text{A3a})$$

since we may close either the ω - or the γ -contour to the right. Therefore, we see Eqs. (A1) are satisfied by use of Eq. (23) and Eqs. (A3).

Appendix B: Constraining a double Laplace image and the homogeneous neighbor functions

Although we have solved the partial differential equation for $\vec{\Gamma}_3(s_{10}, s_{21}, \eta')$, Eq. (27), we need to make sure that any constraints from the integral equation Eq. (14c) are satisfied. To that end, we plug Eqs. (32), (16c) and (26) into Eq. (14c). Doing the s_{32} and η'' integrals, we arrive at the following constraint

$$\begin{aligned} 0 = & \int \frac{d\omega}{2\pi i} \int \frac{d\gamma}{2\pi i} e^{\omega(\eta' - s_{10}) + \gamma s_{10}} \left(\vec{I}_{3\omega\gamma}^{(0)} - G_{2\omega\gamma}^{(0)} + \vec{V}_{\text{UV}} \cdot \vec{I}_{\omega\gamma}^{(0)} \right) \\ & - \int \frac{d\omega}{2\pi i} \int \frac{d\gamma}{2\pi i} e^{\omega(\eta' - s_{21}) + \gamma s_{10}} \left[G_{2\omega\gamma} - G_{2\omega\gamma}^{(0)} - \vec{V}_{\text{UV}} \cdot \left(\vec{I}_{\omega\gamma} - \vec{I}_{\omega\gamma}^{(0)} \right) \right] \\ & + \int \frac{d\omega}{2\pi i} \left\{ \bar{\Gamma}_{3\omega}^+(s_{10}) \left[\frac{e^{s_{10}\delta_{\omega}^+}}{\omega \delta_{\omega}^+} - e^{\delta_{\omega}^+ \eta'} - \frac{e^{\omega(\eta' - s_{21}) + \delta_{\omega}^+ s_{10}}}{\omega \delta_{\omega}^+} \right] + \bar{\Gamma}_{3\omega}^-(s_{10}) \left[\frac{e^{\delta_{\omega}^- s_{10}}}{\omega \delta_{\omega}^-} - e^{\delta_{\omega}^- \eta'} - \frac{e^{\omega(\eta' - s_{21}) + s_{10}\delta_{\omega}^-}}{\omega \delta_{\omega}^-} \right] \right\}, \end{aligned} \quad (\text{B1})$$

where we have made use of the following identities: $\delta_{\omega}^+ \delta_{\omega}^- = 1$, $\delta_{\omega}^+ + \delta_{\omega}^- = \omega$, $(\delta_{\omega}^{\pm})^2 - \omega \delta_{\omega}^{\pm} + 1 = 0$. Now we do the forward Laplace transform over η' to see

$$\begin{aligned} 0 = & \int \frac{d\gamma}{2\pi i} e^{-\omega s_{10} + \gamma s_{10}} \left(\vec{I}_{3\omega\gamma}^{(0)} - G_{2\omega\gamma}^{(0)} + \vec{V}_{\text{UV}} \cdot \vec{I}_{\omega\gamma}^{(0)} \right) \\ & - \int \frac{d\gamma}{2\pi i} e^{-\omega s_{21} + \gamma s_{10}} \left[G_{2\omega\gamma} - G_{2\omega\gamma}^{(0)} - \vec{V}_{\text{UV}} \cdot \left(\vec{I}_{\omega\gamma} - \vec{I}_{\omega\gamma}^{(0)} \right) \right] \\ & - \bar{\Gamma}_{3\omega}^+(s_{10}) \frac{e^{-\omega s_{21} + \delta_{\omega}^+ s_{10}}}{\omega \delta_{\omega}^+} - \bar{\Gamma}_{3\omega}^-(s_{10}) \frac{e^{-\omega s_{21} + \delta_{\omega}^- s_{10}}}{\omega \delta_{\omega}^-} \\ & + \int \frac{d\omega'}{2\pi i} \left(\frac{\bar{\Gamma}_{3\omega'}^+(s_{10})}{\delta_{\omega'}^+ - \omega} + \frac{\bar{\Gamma}_{3\omega'}^-(s_{10})}{\delta_{\omega'}^- - \omega} \right) + \frac{1}{\omega} \int \frac{d\omega'}{2\pi i} \left(\bar{\Gamma}_{3\omega'}^+(s_{10}) \frac{e^{\delta_{\omega'}^+ s_{10}}}{\omega' \delta_{\omega'}^+} + \bar{\Gamma}_{3\omega'}^-(s_{10}) \frac{e^{\delta_{\omega'}^- s_{10}}}{\omega' \delta_{\omega'}^-} \right). \end{aligned} \quad (\text{B2})$$

The second and third lines of Eq. (B2) are dependent on s_{21} , while the first and fourth lines are independent of s_{21} . Since Eq. (B2) is valid for $s_{21} > 0$, we conclude the second and third lines as well as the first and fourth lines must sum to zero separately. Therefore, we have

$$\int \frac{d\gamma}{2\pi i} e^{\gamma s_{10}} \left[G_{2\omega\gamma} - G_{2\omega\gamma}^{(0)} - \vec{V}_{\text{UV}} \cdot \left(\vec{I}_{\omega\gamma} - \vec{I}_{\omega\gamma}^{(0)} \right) \right] + \bar{\Gamma}_{3\omega}^+(s_{10}) \frac{e^{\delta_{\omega}^+ s_{10}}}{\omega \delta_{\omega}^+} + \bar{\Gamma}_{3\omega}^-(s_{10}) \frac{e^{\delta_{\omega}^- s_{10}}}{\omega \delta_{\omega}^-} = 0, \quad (\text{B3a})$$

$$\int \frac{d\gamma}{2\pi i} e^{-\omega s_{10} + \gamma s_{10}} \left(\vec{I}_{3\omega\gamma}^{(0)} - G_{2\omega\gamma}^{(0)} + \vec{V}_{\text{UV}} \cdot \vec{I}_{\omega\gamma}^{(0)} \right) + \int \frac{d\omega'}{2\pi i} \left(\frac{\bar{\Gamma}_{3\omega'}^+(s_{10})}{\delta_{\omega'}^+ - \omega} + \frac{\bar{\Gamma}_{3\omega'}^-(s_{10})}{\delta_{\omega'}^- - \omega} \right) \quad (\text{B3b})$$

$$+\frac{1}{\omega} \int \frac{d\omega'}{2\pi i} \left(\bar{\Gamma}_{3\omega'}^+(s_{10}) \frac{e^{\delta_{\omega'}^+ s_{10}}}{\omega' \delta_{\omega'}^+} + \bar{\Gamma}_{3\omega'}^-(s_{10}) \frac{e^{\delta_{\omega'}^- s_{10}}}{\omega' \delta_{\omega'}^-} \right) = 0.$$

To further constrain the functions $\bar{\Gamma}_{3\omega}^\pm(s_{10})$ and the double Laplace image $\bar{I}_{3\omega\gamma}$, we note from Eq. (14c) we need to satisfy the following boundary condition

$$\bar{\Gamma}_3(s_{10}, s_{21} = s_{10}, \eta') = \bar{I}_3(s_{10}, \eta'). \quad (\text{B4})$$

Substituting Eqs. (21) and (32) into Eq. (B4), and doing the forward Laplace transform over $\eta - s_{10}$, we get

$$\bar{\Gamma}_{3\omega}^+(s_{10}) e^{\delta_{\omega}^+ s_{10}} + \bar{\Gamma}_{3\omega}^-(s_{10}) e^{\delta_{\omega}^- s_{10}} + \int \frac{d\gamma}{2\pi i} e^{\gamma s_{10}} \left(G_{2\omega\gamma} - \vec{V}_{\text{UV}} \cdot \vec{I}_{\omega\gamma} - \bar{I}_{3\omega\gamma} \right) = 0. \quad (\text{B5})$$

With Eqs. (B5) and (B3a), we can solve for $\bar{\Gamma}_{3\omega}^\pm(s_{10})$. We find

$$\bar{\Gamma}_{3\omega}^\pm(s_{10}) = e^{-\delta_{\omega}^\pm s_{10}} \frac{\delta_{\omega}^\pm}{\delta_{\omega}^\pm - \delta_{\omega}^\mp} \int \frac{d\gamma}{2\pi i} e^{\gamma s_{10}} \left\{ (\omega \delta_{\omega}^\mp - 1) \left[G_{2\omega\gamma} - G_{2\omega\gamma}^{(0)} - \vec{V}_{\text{UV}} \cdot (\vec{I}_{\omega\gamma} - \vec{I}_{\omega\gamma}^{(0)}) \right] - G_{2\omega\gamma}^{(0)} + \vec{V}_{\text{UV}} \cdot \vec{I}_{\omega\gamma}^{(0)} + \bar{I}_{3\omega\gamma} \right\}, \quad (\text{B6})$$

which is exactly Eq. (33a) in the main text.

Now we only have to satisfy Eq. (B3b). Using the fact that $G_{2\omega\gamma}, \bar{I}_{3\omega\gamma}, \vec{I}_{\omega\gamma}, \vec{I}_{3\omega\gamma}^{(0)}, G_{2\omega\gamma}^{(0)}, \vec{I}_{\omega\gamma}^{(0)} \rightarrow 0$ as $\omega \rightarrow \infty$, we conclude that $\bar{\Gamma}_{3\omega}^\pm(s_{10}) e^{\delta_{\omega}^\pm s_{10}} \rightarrow 0$ when $\omega \rightarrow \infty$. This fact allows us to close the contour to the right in the last term of Eq. (B3b). We are left with

$$\begin{aligned} \int \frac{d\gamma}{2\pi i} e^{(\gamma-\omega)s_{10}} \left(\vec{I}_{3\omega\gamma}^{(0)} - G_{2\omega\gamma}^{(0)} + \vec{V}_{\text{UV}} \cdot \vec{I}_{\omega\gamma}^{(0)} \right) &= \int \frac{d\omega'}{2\pi i} \left(\frac{\bar{\Gamma}_{3\omega'}^+(s_{10})}{\omega - \delta_{\omega'}^+} + \frac{\bar{\Gamma}_{3\omega'}^-(s_{10})}{\omega - \delta_{\omega'}^-} \right) \\ &= - \int \frac{d\omega'}{2\pi i} \left(\frac{\omega - \delta_{\omega'}^-}{\omega} \frac{\bar{\Gamma}_{3\omega'}^+(s_{10})}{\omega' - (\omega + \frac{1}{\omega})} + \frac{\omega - \delta_{\omega'}^+}{\omega} \frac{\bar{\Gamma}_{3\omega'}^-(s_{10})}{\omega' - (\omega + \frac{1}{\omega})} \right). \end{aligned} \quad (\text{B7})$$

Now we close the contour to the right, picking up the pole at $\omega + \frac{1}{\omega}$. We are left with

$$\int \frac{d\gamma}{2\pi i} e^{\gamma s_{10}} \left(\vec{I}_{3\omega\gamma}^{(0)} - G_{2\omega\gamma}^{(0)} + \vec{V}_{\text{UV}} \cdot \vec{I}_{\omega\gamma}^{(0)} \right) = \left(1 - \frac{1}{\omega^2} \right) \bar{\Gamma}_{3, \omega + \frac{1}{\omega}}^+(s_{10}) e^{\omega s_{10}}. \quad (\text{B8})$$

Using $\delta_{\omega + \frac{1}{\omega}}^+ = \omega$, we can rewrite Eq. (B8) as

$$\int \frac{d\gamma}{2\pi i} e^{\gamma s_{10}} \left(\vec{I}_{3\delta_{\omega + \frac{1}{\omega}}^+ \gamma}^{(0)} - G_{2\delta_{\omega + \frac{1}{\omega}}^+ \gamma}^{(0)} + \vec{V}_{\text{UV}} \cdot \vec{I}_{\delta_{\omega + \frac{1}{\omega}}^+ \gamma}^{(0)} \right) = \left(1 - \frac{1}{[\delta_{\omega + \frac{1}{\omega}}^+]^2} \right) \bar{\Gamma}_{3, \omega + \frac{1}{\omega}}^+(s_{10}) e^{\delta_{\omega + \frac{1}{\omega}}^+ s_{10}}, \quad (\text{B9})$$

and, upon replacing $\omega + \frac{1}{\omega} \rightarrow \omega$, we have

$$\int \frac{d\gamma}{2\pi i} e^{\gamma s_{10}} \left(\vec{I}_{3\delta_{\omega}^+ \gamma}^{(0)} - G_{2\delta_{\omega}^+ \gamma}^{(0)} + \vec{V}_{\text{UV}} \cdot \vec{I}_{\delta_{\omega}^+ \gamma}^{(0)} \right) = \left(1 - \frac{1}{[\delta_{\omega}^+]^2} \right) \bar{\Gamma}_{3, \omega}^+(s_{10}) e^{\delta_{\omega}^+ s_{10}}. \quad (\text{B10})$$

Employing Eq. (B6), and doing the forward Laplace transform over s_{10} , we find

$$\vec{I}_{3\delta_{\omega}^+ \gamma}^{(0)} - G_{2\delta_{\omega}^+ \gamma}^{(0)} + \vec{V}_{\text{UV}} \cdot \vec{I}_{\delta_{\omega}^+ \gamma}^{(0)} = (\omega \delta_{\omega}^\mp - 1) \left[G_{2\omega\gamma} - G_{2\omega\gamma}^{(0)} - \vec{V}_{\text{UV}} \cdot (\vec{I}_{\omega\gamma} - \vec{I}_{\omega\gamma}^{(0)}) \right] - G_{2\omega\gamma}^{(0)} + \vec{V}_{\text{UV}} \cdot \vec{I}_{\omega\gamma}^{(0)} + \bar{I}_{3\omega\gamma}. \quad (\text{B11})$$

Via Eqs. (23), we can solve for $\bar{I}_{3\omega\gamma}$ explicitly. We get

$$\begin{aligned} \bar{I}_{3\omega\gamma} &= \frac{\vec{V}_{\text{UV}} \cdot (\vec{I}_{\omega\gamma}^{(0)} - \vec{I}_{\delta_{\omega}^+ \gamma}^{(0)}) - G_{2\omega\gamma}^{(0)} + G_{2\delta_{\omega}^+ \gamma}^{(0)} - \vec{I}_{3\delta_{\omega}^+ \gamma}^{(0)}}{(\omega \delta_{\omega}^- - 1) \vec{V}_{\text{UV}} \cdot (2\omega\gamma - M_{\text{IR}})^{-1} \vec{V}_{\bar{I}_3} - 1} \\ &\quad + \frac{(\omega \delta_{\omega}^- - 1) \left[G_{2\omega\gamma} - G_{2\omega\gamma}^{(0)} + \vec{V}_{\text{UV}} \cdot \vec{I}_{\omega\gamma}^{(0)} - \vec{V}_{\text{UV}} \cdot (2\omega\gamma - M_{\text{IR}})^{-1} (2\omega\gamma \vec{I}_{\omega\gamma}^{(0)} + G_{\omega\gamma} \vec{V}_G + G_{2\omega\gamma} \vec{V}_{G_2}) \right]}{(\omega \delta_{\omega}^- - 1) \vec{V}_{\text{UV}} \cdot (2\omega\gamma - M_{\text{IR}})^{-1} \vec{V}_{\bar{I}_3} - 1}, \end{aligned} \quad (\text{B12})$$

which is exactly Eq. (33b) in the main text.

Appendix C: Exact expressions for the asymptotic OAM to helicity PDF ratios

Here we give the exact expressions for the asymptotic ratios, $R_q(t), R_G(t)$, in Eqs. (49) using the branch cut discontinuity approximation outlined in the main text. Let us start with the quark OAM to quark hPDF ratio. First, we denote the coefficient $R_q(t)$ in Eqs. (49) by

$$R_q(t) = \frac{N_q(t)}{D_q(t)}. \quad (C1)$$

Then, using the procedure to obtain $R_q(t)$ outlined in the main text, we find

$$\begin{aligned} N_q(t) = & 3e^{\frac{1}{32}t\omega_b(\omega_b^2+16)-\frac{5t}{2\omega_b}}p_{\omega_b}\omega_b^{46} + 720e^{\frac{1}{32}t\omega_b(\omega_b^2+16)-\frac{5t}{2\omega_b}}p_{\omega_b}\omega_b^{44} + 51744e^{\frac{1}{32}t\omega_b(\omega_b^2+16)-\frac{5t}{2\omega_b}}p_{\omega_b}\omega_b^{42} \\ & - 2048e^{\frac{t\omega_b^3}{32}+t\omega_b-\frac{5t}{2\omega_b}}tp_{\omega_b}\omega_b^{41} - 4096e^{\frac{t\omega_b^3}{32}+t\omega_b-\frac{5t}{2\omega_b}}p_{\omega_b}\omega_b^{40} + 573696e^{\frac{1}{32}t\omega_b(\omega_b^2+16)-\frac{5t}{2\omega_b}}p_{\omega_b}\omega_b^{40} \\ & - 494080e^{\frac{t\omega_b^3}{32}+t\omega_b-\frac{5t}{2\omega_b}}tp_{\omega_b}\omega_b^{39} - 25165824\sqrt{2}e^{\frac{t(\omega_b^4+48\omega_b^2-4\sqrt{2}p_{\omega_b}+80)}{64\omega_b}-\frac{5t}{2\omega_b}}\omega_b^{38} - 1007616e^{\frac{t\omega_b^3}{32}+t\omega_b-\frac{5t}{2\omega_b}}p_{\omega_b}\omega_b^{38} \\ & - 52880640e^{\frac{1}{32}t\omega_b(\omega_b^2+16)-\frac{5t}{2\omega_b}}p_{\omega_b}\omega_b^{38} + 25165824e^{\frac{t(\omega_b^4+48\omega_b^2-4\sqrt{2}p_{\omega_b}+80)}{64\omega_b}-\frac{5t}{2\omega_b}}\sqrt{2}\omega_b^{38} - 36444160e^{\frac{t\omega_b^3}{32}+t\omega_b-\frac{5t}{2\omega_b}}tp_{\omega_b}\omega_b^{37} \\ & - 767557632\sqrt{2}e^{\frac{t(\omega_b^4+48\omega_b^2-4\sqrt{2}p_{\omega_b}+80)}{64\omega_b}-\frac{5t}{2\omega_b}}\omega_b^{36} - 77893632e^{\frac{t\omega_b^3}{32}+t\omega_b-\frac{5t}{2\omega_b}}p_{\omega_b}\omega_b^{36} \\ & - 2097152e^{\frac{t(\omega_b^4+48\omega_b^2-4\sqrt{2}p_{\omega_b}+80)}{64\omega_b}-\frac{5t}{2\omega_b}}p_{\omega_b}\omega_b^{36} - 2097152e^{\frac{t(\omega_b^4+48\omega_b^2-4\sqrt{2}p_{\omega_b}+80)}{64\omega_b}-\frac{5t}{2\omega_b}}p_{\omega_b}\omega_b^{36} \\ & - 710320128e^{\frac{1}{32}t\omega_b(\omega_b^2+16)-\frac{5t}{2\omega_b}}p_{\omega_b}\omega_b^{36} + 767557632e^{\frac{t(\omega_b^4+48\omega_b^2-4\sqrt{2}p_{\omega_b}+80)}{64\omega_b}-\frac{5t}{2\omega_b}}\sqrt{2}\omega_b^{36} \\ & - 559202304e^{\frac{t\omega_b^3}{32}+t\omega_b-\frac{5t}{2\omega_b}}tp_{\omega_b}\omega_b^{35} - 3825205248\sqrt{2}e^{\frac{t(\omega_b^4+48\omega_b^2-4\sqrt{2}p_{\omega_b}+80)}{64\omega_b}-\frac{5t}{2\omega_b}}\omega_b^{34} - 1543700480e^{\frac{t\omega_b^3}{32}+t\omega_b-\frac{5t}{2\omega_b}}p_{\omega_b}\omega_b^{34} \\ & + 33554432e^{\frac{t(\omega_b^4+48\omega_b^2-4\sqrt{2}p_{\omega_b}+80)}{64\omega_b}-\frac{5t}{2\omega_b}}p_{\omega_b}\omega_b^{34} + 33554432e^{\frac{t(\omega_b^4+48\omega_b^2-4\sqrt{2}p_{\omega_b}+80)}{64\omega_b}-\frac{5t}{2\omega_b}}p_{\omega_b}\omega_b^{34} \\ & + 24862507008e^{\frac{1}{32}t\omega_b(\omega_b^2+16)-\frac{5t}{2\omega_b}}p_{\omega_b}\omega_b^{34} + 3825205248e^{\frac{t(\omega_b^4+48\omega_b^2-4\sqrt{2}p_{\omega_b}+80)}{64\omega_b}-\frac{5t}{2\omega_b}}\sqrt{2}\omega_b^{34} \\ & + 26303004672e^{\frac{t\omega_b^3}{32}+t\omega_b-\frac{5t}{2\omega_b}}tp_{\omega_b}\omega_b^{33} - 523851792384\sqrt{2}e^{\frac{t(\omega_b^4+48\omega_b^2-4\sqrt{2}p_{\omega_b}+80)}{64\omega_b}-\frac{5t}{2\omega_b}}\omega_b^{32} \\ & + 40762867712e^{\frac{t\omega_b^3}{32}+t\omega_b-\frac{5t}{2\omega_b}}p_{\omega_b}\omega_b^{32} - 738197504e^{\frac{t(\omega_b^4+48\omega_b^2-4\sqrt{2}p_{\omega_b}+80)}{64\omega_b}-\frac{5t}{2\omega_b}}p_{\omega_b}\omega_b^{32} \\ & - 738197504e^{\frac{t(\omega_b^4+48\omega_b^2-4\sqrt{2}p_{\omega_b}+80)}{64\omega_b}-\frac{5t}{2\omega_b}}p_{\omega_b}\omega_b^{32} + 213254406144e^{\frac{1}{32}t\omega_b(\omega_b^2+16)-\frac{5t}{2\omega_b}}p_{\omega_b}\omega_b^{32} \\ & + 523851792384e^{\frac{t(\omega_b^4+48\omega_b^2-4\sqrt{2}p_{\omega_b}+80)}{64\omega_b}-\frac{5t}{2\omega_b}}\sqrt{2}\omega_b^{32} + 373427273728e^{\frac{t\omega_b^3}{32}+t\omega_b-\frac{5t}{2\omega_b}}tp_{\omega_b}\omega_b^{31} \\ & - 5399847632896\sqrt{2}e^{\frac{t(\omega_b^4+48\omega_b^2-4\sqrt{2}p_{\omega_b}+80)}{64\omega_b}-\frac{5t}{2\omega_b}}\omega_b^{30} + 831344607232e^{\frac{t\omega_b^3}{32}+t\omega_b-\frac{5t}{2\omega_b}}p_{\omega_b}\omega_b^{30} \\ & - 27380416512e^{\frac{t(\omega_b^4+48\omega_b^2-4\sqrt{2}p_{\omega_b}+80)}{64\omega_b}-\frac{5t}{2\omega_b}}p_{\omega_b}\omega_b^{30} - 27380416512e^{\frac{t(\omega_b^4+48\omega_b^2-4\sqrt{2}p_{\omega_b}+80)}{64\omega_b}-\frac{5t}{2\omega_b}}p_{\omega_b}\omega_b^{30} \\ & - 6494217043968e^{\frac{1}{32}t\omega_b(\omega_b^2+16)-\frac{5t}{2\omega_b}}p_{\omega_b}\omega_b^{30} + 5399847632896e^{\frac{t(\omega_b^4+48\omega_b^2-4\sqrt{2}p_{\omega_b}+80)}{64\omega_b}-\frac{5t}{2\omega_b}}\sqrt{2}\omega_b^{30} \\ & - 9810711937024e^{\frac{t\omega_b^3}{32}+t\omega_b-\frac{5t}{2\omega_b}}tp_{\omega_b}\omega_b^{29} - 151795955400704\sqrt{2}e^{\frac{t(\omega_b^4+48\omega_b^2-4\sqrt{2}p_{\omega_b}+80)}{64\omega_b}-\frac{5t}{2\omega_b}}\omega_b^{28} \\ & - 14009780666368e^{\frac{t\omega_b^3}{32}+t\omega_b-\frac{5t}{2\omega_b}}p_{\omega_b}\omega_b^{28} + 2406792298496e^{\frac{t(\omega_b^4+48\omega_b^2-4\sqrt{2}p_{\omega_b}+80)}{64\omega_b}-\frac{5t}{2\omega_b}}p_{\omega_b}\omega_b^{28} \\ & + 2406792298496e^{\frac{t(\omega_b^4+48\omega_b^2-4\sqrt{2}p_{\omega_b}+80)}{64\omega_b}-\frac{5t}{2\omega_b}}p_{\omega_b}\omega_b^{28} - 21791590318080e^{\frac{1}{32}t\omega_b(\omega_b^2+16)-\frac{5t}{2\omega_b}}p_{\omega_b}\omega_b^{28} \\ & + 151795955400704e^{\frac{t(\omega_b^4+48\omega_b^2-4\sqrt{2}p_{\omega_b}+80)}{64\omega_b}-\frac{5t}{2\omega_b}}\sqrt{2}\omega_b^{28} - 50353122836480e^{\frac{t\omega_b^3}{32}+t\omega_b-\frac{5t}{2\omega_b}}tp_{\omega_b}\omega_b^{27} \\ & - 741861111103488\sqrt{2}e^{\frac{t(\omega_b^4+48\omega_b^2-4\sqrt{2}p_{\omega_b}+80)}{64\omega_b}-\frac{5t}{2\omega_b}}\omega_b^{26} - 107827301449728e^{\frac{t\omega_b^3}{32}+t\omega_b-\frac{5t}{2\omega_b}}p_{\omega_b}\omega_b^{26} \\ & + 4140348473344e^{\frac{t(\omega_b^4+48\omega_b^2-4\sqrt{2}p_{\omega_b}+80)}{64\omega_b}-\frac{5t}{2\omega_b}}p_{\omega_b}\omega_b^{26} + 4140348473344e^{\frac{t(\omega_b^4+48\omega_b^2-4\sqrt{2}p_{\omega_b}+80)}{64\omega_b}-\frac{5t}{2\omega_b}}p_{\omega_b}\omega_b^{26} \end{aligned} \quad (C2a)$$

$$\begin{aligned}
& + 934671588261888e^{\frac{1}{32}t\omega_b(\omega_b^2+16)-\frac{5t}{2\omega_b}p_{\omega_b}\omega_b^{26}} + 741861111103488e^{\frac{t(\omega_b^4+48\omega_b^2+4p_{\omega_b}\sqrt{2}+80)}{64\omega_b}-\frac{5t}{2\omega_b}\sqrt{2}\omega_b^{26}} \\
& + 1752851315425280e^{\frac{t\omega_b^3}{32}+t\omega_b-\frac{5t}{2\omega_b}tp_{\omega_b}\omega_b^{25}} - 17967050790010880\sqrt{2}e^{\frac{t(\omega_b^4+48\omega_b^2+4p_{\omega_b}\sqrt{2}+80)}{64\omega_b}-\frac{5t}{2\omega_b}\omega_b^{24}} \\
& + 2561436890955776e^{\frac{t\omega_b^3}{32}+t\omega_b-\frac{5t}{2\omega_b}p_{\omega_b}\omega_b^{24}} - 764882135810048e^{\frac{t(\omega_b^4+48\omega_b^2+4p_{\omega_b}\sqrt{2}+80)}{64\omega_b}-\frac{5t}{2\omega_b}p_{\omega_b}\omega_b^{24}} \\
& - 764882135810048e^{\frac{t(\omega_b^4+48\omega_b^2-4\sqrt{2}p_{\omega_b}+80)}{64\omega_b}-\frac{5t}{2\omega_b}p_{\omega_b}\omega_b^{24}} - 301558243786752e^{\frac{1}{32}t\omega_b(\omega_b^2+16)-\frac{5t}{2\omega_b}p_{\omega_b}\omega_b^{24}} \\
& + 17967050790010880e^{\frac{t(\omega_b^4+48\omega_b^2-4\sqrt{2}p_{\omega_b}+80)}{64\omega_b}-\frac{5t}{2\omega_b}\sqrt{2}\omega_b^{24}} - 3616723240484864e^{\frac{t\omega_b^3}{32}+t\omega_b-\frac{5t}{2\omega_b}tp_{\omega_b}\omega_b^{23}} \\
& - 27413023903711232\sqrt{2}e^{\frac{t(\omega_b^4+48\omega_b^2+4p_{\omega_b}\sqrt{2}+80)}{64\omega_b}-\frac{5t}{2\omega_b}\omega_b^{22}} - 5950350771093504e^{\frac{t\omega_b^3}{32}+t\omega_b-\frac{5t}{2\omega_b}p_{\omega_b}\omega_b^{22}} \\
& + 1801000046297088e^{\frac{t(\omega_b^4+48\omega_b^2+4p_{\omega_b}\sqrt{2}+80)}{64\omega_b}-\frac{5t}{2\omega_b}p_{\omega_b}\omega_b^{22}} + 1801000046297088e^{\frac{t(\omega_b^4+48\omega_b^2-4\sqrt{2}p_{\omega_b}+80)}{64\omega_b}-\frac{5t}{2\omega_b}p_{\omega_b}\omega_b^{22}} \\
& - 72638222076739584e^{\frac{1}{32}t\omega_b(\omega_b^2+16)-\frac{5t}{2\omega_b}p_{\omega_b}\omega_b^{22}} + 27413023903711232e^{\frac{t(\omega_b^4+48\omega_b^2-4\sqrt{2}p_{\omega_b}+80)}{64\omega_b}-\frac{5t}{2\omega_b}\sqrt{2}\omega_b^{22}} \\
& - 97407659250024448e^{\frac{t\omega_b^3}{32}+t\omega_b-\frac{5t}{2\omega_b}tp_{\omega_b}\omega_b^{21}} - 817908008204894208\sqrt{2}e^{\frac{t(\omega_b^4+48\omega_b^2-4\sqrt{2}p_{\omega_b}+80)}{64\omega_b}-\frac{5t}{2\omega_b}\omega_b^{20}} \\
& - 140594551843717120e^{\frac{t\omega_b^3}{32}+t\omega_b-\frac{5t}{2\omega_b}p_{\omega_b}\omega_b^{20}} + 85902094699069440e^{\frac{t(\omega_b^4+48\omega_b^2+4p_{\omega_b}\sqrt{2}+80)}{64\omega_b}-\frac{5t}{2\omega_b}p_{\omega_b}\omega_b^{20}} \\
& + 85902094699069440e^{\frac{t(\omega_b^4+48\omega_b^2-4\sqrt{2}p_{\omega_b}+80)}{64\omega_b}-\frac{5t}{2\omega_b}p_{\omega_b}\omega_b^{20}} + 210661754957463552e^{\frac{1}{32}t\omega_b(\omega_b^2+16)-\frac{5t}{2\omega_b}p_{\omega_b}\omega_b^{20}} \\
& + 817908008204894208e^{\frac{t(\omega_b^4+48\omega_b^2+4p_{\omega_b}\sqrt{2}+80)}{64\omega_b}-\frac{5t}{2\omega_b}\sqrt{2}\omega_b^{20}} + 621934354204983296e^{\frac{t\omega_b^3}{32}+t\omega_b-\frac{5t}{2\omega_b}tp_{\omega_b}\omega_b^{19}} \\
& - 811421989112643584\sqrt{2}e^{\frac{t(\omega_b^4+48\omega_b^2-4\sqrt{2}p_{\omega_b}+80)}{64\omega_b}-\frac{5t}{2\omega_b}\omega_b^{18}} + 1225955464970240000e^{\frac{t\omega_b^3}{32}+t\omega_b-\frac{5t}{2\omega_b}p_{\omega_b}\omega_b^{18}} \\
& - 404796200882012160e^{\frac{t(\omega_b^4+48\omega_b^2+4p_{\omega_b}\sqrt{2}+80)}{64\omega_b}-\frac{5t}{2\omega_b}p_{\omega_b}\omega_b^{18}} - 404796200882012160e^{\frac{t(\omega_b^4+48\omega_b^2-4\sqrt{2}p_{\omega_b}+80)}{64\omega_b}-\frac{5t}{2\omega_b}p_{\omega_b}\omega_b^{18}} \\
& + 2786186654040195072e^{\frac{1}{32}t\omega_b(\omega_b^2+16)-\frac{5t}{2\omega_b}p_{\omega_b}\omega_b^{18}} + 811421989112643584e^{\frac{t(\omega_b^4+48\omega_b^2+4p_{\omega_b}\sqrt{2}+80)}{64\omega_b}-\frac{5t}{2\omega_b}\sqrt{2}\omega_b^{18}} \\
& - 352230748981297152e^{\frac{t\omega_b^3}{32}+t\omega_b-\frac{5t}{2\omega_b}tp_{\omega_b}\omega_b^{17}} - 11789614583897915392\sqrt{2}e^{\frac{t(\omega_b^4+48\omega_b^2+4p_{\omega_b}\sqrt{2}+80)}{64\omega_b}-\frac{5t}{2\omega_b}\omega_b^{16}} \\
& - 1120551882285121536e^{\frac{t\omega_b^3}{32}+t\omega_b-\frac{5t}{2\omega_b}p_{\omega_b}\omega_b^{16}} - 3398089064153350144e^{\frac{t(\omega_b^4+48\omega_b^2+4p_{\omega_b}\sqrt{2}+80)}{64\omega_b}-\frac{5t}{2\omega_b}p_{\omega_b}\omega_b^{16}} \\
& - 3398089064153350144e^{\frac{t(\omega_b^4+48\omega_b^2-4\sqrt{2}p_{\omega_b}+80)}{64\omega_b}-\frac{5t}{2\omega_b}p_{\omega_b}\omega_b^{16}} - 14601690338725724160e^{\frac{1}{32}t\omega_b(\omega_b^2+16)-\frac{5t}{2\omega_b}p_{\omega_b}\omega_b^{16}} \\
& + 11789614583897915392e^{\frac{t(\omega_b^4+48\omega_b^2-4\sqrt{2}p_{\omega_b}+80)}{64\omega_b}-\frac{5t}{2\omega_b}\sqrt{2}\omega_b^{16}} - 13657447344977739776e^{\frac{t\omega_b^3}{32}+t\omega_b-\frac{5t}{2\omega_b}tp_{\omega_b}\omega_b^{15}} \\
& - 84602933749921873920\sqrt{2}e^{\frac{t(\omega_b^4+48\omega_b^2+4p_{\omega_b}\sqrt{2}+80)}{64\omega_b}-\frac{5t}{2\omega_b}\omega_b^{14}} - 36435246885334155264e^{\frac{t\omega_b^3}{32}+t\omega_b-\frac{5t}{2\omega_b}p_{\omega_b}\omega_b^{14}} \\
& + 24123812878986772480e^{\frac{t(\omega_b^4+48\omega_b^2+4p_{\omega_b}\sqrt{2}+80)}{64\omega_b}-\frac{5t}{2\omega_b}p_{\omega_b}\omega_b^{14}} + 24123812878986772480e^{\frac{t(\omega_b^4+48\omega_b^2-4\sqrt{2}p_{\omega_b}+80)}{64\omega_b}-\frac{5t}{2\omega_b}p_{\omega_b}\omega_b^{14}} \\
& - 34005836361344483328e^{\frac{1}{32}t\omega_b(\omega_b^2+16)-\frac{5t}{2\omega_b}p_{\omega_b}\omega_b^{14}} + 84602933749921873920e^{\frac{t(\omega_b^4+48\omega_b^2-4\sqrt{2}p_{\omega_b}+80)}{64\omega_b}-\frac{5t}{2\omega_b}\sqrt{2}\omega_b^{14}} \\
& + 114882322894593982464e^{\frac{t\omega_b^3}{32}+t\omega_b-\frac{5t}{2\omega_b}tp_{\omega_b}\omega_b^{13}} - 309548164987869986816\sqrt{2}e^{\frac{t(\omega_b^4+48\omega_b^2-4\sqrt{2}p_{\omega_b}+80)}{64\omega_b}-\frac{5t}{2\omega_b}\omega_b^{12}} \\
& + 204931797443867049984e^{\frac{t\omega_b^3}{32}+t\omega_b-\frac{5t}{2\omega_b}p_{\omega_b}\omega_b^{12}} + 6423258968537169920e^{\frac{t(\omega_b^4+48\omega_b^2+4p_{\omega_b}\sqrt{2}+80)}{64\omega_b}-\frac{5t}{2\omega_b}p_{\omega_b}\omega_b^{12}} \\
& + 6423258968537169920e^{\frac{t(\omega_b^4+48\omega_b^2-4\sqrt{2}p_{\omega_b}+80)}{64\omega_b}-\frac{5t}{2\omega_b}p_{\omega_b}\omega_b^{12}} + 370695788928492896256e^{\frac{1}{32}t\omega_b(\omega_b^2+16)-\frac{5t}{2\omega_b}p_{\omega_b}\omega_b^{12}} \\
& + 309548164987869986816e^{\frac{t(\omega_b^4+48\omega_b^2+4p_{\omega_b}\sqrt{2}+80)}{64\omega_b}-\frac{5t}{2\omega_b}\sqrt{2}\omega_b^{12}} \\
& - 359423279061184544768e^{\frac{t\omega_b^3}{32}+t\omega_b-\frac{5t}{2\omega_b}tp_{\omega_b}\omega_b^{11}} - 868402094548088520704\sqrt{2}e^{\frac{t(\omega_b^4+48\omega_b^2-4\sqrt{2}p_{\omega_b}+80)}{64\omega_b}-\frac{5t}{2\omega_b}\omega_b^{10}}
\end{aligned}$$

$$\begin{aligned}
& -267333673880712642560e^{\frac{t\omega_b^3}{32}+t\omega_b-\frac{5t}{2\omega_b}}p_{\omega_b}\omega_b^{10} - 325394080276773076992e^{\frac{t(\omega_b^4+48\omega_b^2+4p_{\omega_b}\sqrt{2}+80)}{64\omega_b}-\frac{5t}{2\omega_b}}p_{\omega_b}\omega_b^{10} \\
& - 325394080276773076992e^{\frac{t(\omega_b^4+48\omega_b^2-4\sqrt{2}p_{\omega_b}+80)}{64\omega_b}-\frac{5t}{2\omega_b}}p_{\omega_b}\omega_b^{10} - 545782231641775669248e^{\frac{1}{32}t\omega_b(\omega_b^2+16)-\frac{5t}{2\omega_b}}p_{\omega_b}\omega_b^{10} \\
& + 868402094548088520704e^{\frac{t(\omega_b^4+48\omega_b^2+4p_{\omega_b}\sqrt{2}+80)}{64\omega_b}-\frac{5t}{2\omega_b}}\sqrt{2}\omega_b^{10} - 504547273453571407872e^{\frac{t\omega_b^3}{32}+t\omega_b-\frac{5t}{2\omega_b}}tp_{\omega_b}\omega_b^9 \\
& - 4440188944617119416320\sqrt{2}e^{\frac{t(\omega_b^4+48\omega_b^2+4p_{\omega_b}\sqrt{2}+80)}{64\omega_b}-\frac{5t}{2\omega_b}}\omega_b^8 - 1566532094384553328640e^{\frac{t\omega_b^3}{32}+t\omega_b-\frac{5t}{2\omega_b}}p_{\omega_b}\omega_b^8 \\
& + 772601523274663329792e^{\frac{t(\omega_b^4+48\omega_b^2+4p_{\omega_b}\sqrt{2}+80)}{64\omega_b}-\frac{5t}{2\omega_b}}p_{\omega_b}\omega_b^8 + 772601523274663329792e^{\frac{t(\omega_b^4+48\omega_b^2-4\sqrt{2}p_{\omega_b}+80)}{64\omega_b}-\frac{5t}{2\omega_b}}p_{\omega_b}\omega_b^8 \\
& - 2130598940513453211648e^{\frac{1}{32}t\omega_b(\omega_b^2+16)-\frac{5t}{2\omega_b}}p_{\omega_b}\omega_b^8 + 4440188944617119416320e^{\frac{t(\omega_b^4+48\omega_b^2-4\sqrt{2}p_{\omega_b}+80)}{64\omega_b}-\frac{5t}{2\omega_b}}\sqrt{2}\omega_b^8 \\
& + 6245375790455290068992e^{\frac{t\omega_b^3}{32}+t\omega_b-\frac{5t}{2\omega_b}}tp_{\omega_b}\omega_b^7 - 5688514703730182979584\sqrt{2}e^{\frac{t(\omega_b^4+48\omega_b^2-4\sqrt{2}p_{\omega_b}+80)}{64\omega_b}-\frac{5t}{2\omega_b}}p_{\omega_b}\omega_b^6 \\
& + 8388656867519418597376e^{\frac{t\omega_b^3}{32}+t\omega_b-\frac{5t}{2\omega_b}}p_{\omega_b}\omega_b^6 - 616813004964663132160e^{\frac{t(\omega_b^4+48\omega_b^2+4p_{\omega_b}\sqrt{2}+80)}{64\omega_b}-\frac{5t}{2\omega_b}}p_{\omega_b}\omega_b^6 \\
& - 616813004964663132160e^{\frac{t(\omega_b^4+48\omega_b^2-4\sqrt{2}p_{\omega_b}+80)}{64\omega_b}-\frac{5t}{2\omega_b}}p_{\omega_b}\omega_b^6 + 9477014767868282142720e^{\frac{1}{32}t\omega_b(\omega_b^2+16)-\frac{5t}{2\omega_b}}p_{\omega_b}\omega_b^6 \\
& + 5688514703730182979584e^{\frac{t(\omega_b^4+48\omega_b^2+4p_{\omega_b}\sqrt{2}+80)}{64\omega_b}-\frac{5t}{2\omega_b}}\sqrt{2}\omega_b^6 - 16002550483943036026880e^{\frac{t\omega_b^3}{32}+t\omega_b-\frac{5t}{2\omega_b}}tp_{\omega_b}\omega_b^5 \\
& - 2287396265139984400384\sqrt{2}e^{\frac{t(\omega_b^4+48\omega_b^2+4p_{\omega_b}\sqrt{2}+80)}{64\omega_b}-\frac{5t}{2\omega_b}}\omega_b^4 - 17764214542982298206208e^{\frac{t\omega_b^3}{32}+t\omega_b-\frac{5t}{2\omega_b}}p_{\omega_b}\omega_b^4 \\
& + 110680464442257309696e^{\frac{t(\omega_b^4+48\omega_b^2+4p_{\omega_b}\sqrt{2}+80)}{64\omega_b}-\frac{5t}{2\omega_b}}p_{\omega_b}\omega_b^4 + 110680464442257309696e^{\frac{t(\omega_b^4+48\omega_b^2-4\sqrt{2}p_{\omega_b}+80)}{64\omega_b}-\frac{5t}{2\omega_b}}p_{\omega_b}\omega_b^4 \\
& - 15329244325252637392896e^{\frac{1}{32}t\omega_b(\omega_b^2+16)-\frac{5t}{2\omega_b}}p_{\omega_b}\omega_b^4 + 2287396265139984400384e^{\frac{t(\omega_b^4+48\omega_b^2-4\sqrt{2}p_{\omega_b}+80)}{64\omega_b}-\frac{5t}{2\omega_b}}\sqrt{2}\omega_b^4 \\
& + 17487513381876654931968e^{\frac{t\omega_b^3}{32}+t\omega_b-\frac{5t}{2\omega_b}}tp_{\omega_b}\omega_b^3 + 18004022215940522377216e^{\frac{t\omega_b^3}{32}+t\omega_b-\frac{5t}{2\omega_b}}p_{\omega_b}\omega_b^2 \\
& + 11732129230879274827776e^{\frac{1}{32}t\omega_b(\omega_b^2+16)-\frac{5t}{2\omega_b}}p_{\omega_b}\omega_b^2 - 7083549724304467820544e^{\frac{t\omega_b^3}{32}+t\omega_b-\frac{5t}{2\omega_b}}tp_{\omega_b}\omega_b \\
& - 7083549724304467820544e^{\frac{t\omega_b^3}{32}+t\omega_b-\frac{5t}{2\omega_b}}p_{\omega_b} - 3541774862152233910272e^{\frac{1}{32}t\omega_b(\omega_b^2+16)-\frac{5t}{2\omega_b}}p_{\omega_b}, \\
D_q(t) = & 16e^{\frac{t\omega_b^3}{32}+t\omega_b-\frac{5t}{2\omega_b}}tp_{\omega_b}\omega_b^{45} + 32e^{\frac{t\omega_b^3}{32}+t\omega_b-\frac{5t}{2\omega_b}}p_{\omega_b}\omega_b^{44} + 4096e^{\frac{t\omega_b^3}{32}+t\omega_b-\frac{5t}{2\omega_b}}tp_{\omega_b}\omega_b^{43} + 8192e^{\frac{t\omega_b^3}{32}+t\omega_b-\frac{5t}{2\omega_b}}p_{\omega_b}\omega_b^{42} \\
& + 341504e^{\frac{t\omega_b^3}{32}+t\omega_b-\frac{5t}{2\omega_b}}tp_{\omega_b}\omega_b^{41} + 683008e^{\frac{t\omega_b^3}{32}+t\omega_b-\frac{5t}{2\omega_b}}p_{\omega_b}\omega_b^{40} + 8523776e^{\frac{t\omega_b^3}{32}+t\omega_b-\frac{5t}{2\omega_b}}tp_{\omega_b}\omega_b^{39} \\
& + 17047552e^{\frac{t\omega_b^3}{32}+t\omega_b-\frac{5t}{2\omega_b}}p_{\omega_b}\omega_b^{38} - 145649664e^{\frac{t\omega_b^3}{32}+t\omega_b-\frac{5t}{2\omega_b}}tp_{\omega_b}\omega_b^{37} - 291299328e^{\frac{t\omega_b^3}{32}+t\omega_b-\frac{5t}{2\omega_b}}p_{\omega_b}\omega_b^{36} \\
& - 6118768640e^{\frac{t\omega_b^3}{32}+t\omega_b-\frac{5t}{2\omega_b}}tp_{\omega_b}\omega_b^{35} - 12237537280e^{\frac{t\omega_b^3}{32}+t\omega_b-\frac{5t}{2\omega_b}}p_{\omega_b}\omega_b^{34} + 34699739136e^{\frac{t\omega_b^3}{32}+t\omega_b-\frac{5t}{2\omega_b}}tp_{\omega_b}\omega_b^{33} \\
& + 69399478272e^{\frac{t\omega_b^3}{32}+t\omega_b-\frac{5t}{2\omega_b}}p_{\omega_b}\omega_b^{32} + 1692552658944e^{\frac{t\omega_b^3}{32}+t\omega_b-\frac{5t}{2\omega_b}}tp_{\omega_b}\omega_b^{31} + 3385105317888e^{\frac{t\omega_b^3}{32}+t\omega_b-\frac{5t}{2\omega_b}}p_{\omega_b}\omega_b^{30} \\
& - 7554981691392e^{\frac{t\omega_b^3}{32}+t\omega_b-\frac{5t}{2\omega_b}}tp_{\omega_b}\omega_b^{29} - 15109963382784e^{\frac{t\omega_b^3}{32}+t\omega_b-\frac{5t}{2\omega_b}}p_{\omega_b}\omega_b^{28} \\
& - 237101522092032e^{\frac{t\omega_b^3}{32}+t\omega_b-\frac{5t}{2\omega_b}}tp_{\omega_b}\omega_b^{27} - 474203044184064e^{\frac{t\omega_b^3}{32}+t\omega_b-\frac{5t}{2\omega_b}}p_{\omega_b}\omega_b^{26} \\
& + 1191290783924224e^{\frac{t\omega_b^3}{32}+t\omega_b-\frac{5t}{2\omega_b}}tp_{\omega_b}\omega_b^{25} + 2382581567848448e^{\frac{t\omega_b^3}{32}+t\omega_b-\frac{5t}{2\omega_b}}p_{\omega_b}\omega_b^{24} \\
& + 17452341909258240e^{\frac{t\omega_b^3}{32}+t\omega_b-\frac{5t}{2\omega_b}}tp_{\omega_b}\omega_b^{23} + 34904683818516480e^{\frac{t\omega_b^3}{32}+t\omega_b-\frac{5t}{2\omega_b}}p_{\omega_b}\omega_b^{22} \\
& - 108166380527812608e^{\frac{t\omega_b^3}{32}+t\omega_b-\frac{5t}{2\omega_b}}tp_{\omega_b}\omega_b^{21} - 216332761055625216e^{\frac{t\omega_b^3}{32}+t\omega_b-\frac{5t}{2\omega_b}}p_{\omega_b}\omega_b^{20} \\
& - 607132728671862784e^{\frac{t\omega_b^3}{32}+t\omega_b-\frac{5t}{2\omega_b}}tp_{\omega_b}\omega_b^{19} - 1214265457343725568e^{\frac{t\omega_b^3}{32}+t\omega_b-\frac{5t}{2\omega_b}}p_{\omega_b}\omega_b^{18} \\
& + 5145538496131235840e^{\frac{t\omega_b^3}{32}+t\omega_b-\frac{5t}{2\omega_b}}tp_{\omega_b}\omega_b^{17} + 10291076992262471680e^{\frac{t\omega_b^3}{32}+t\omega_b-\frac{5t}{2\omega_b}}p_{\omega_b}\omega_b^{16}
\end{aligned} \tag{C2b}$$

$$\begin{aligned}
& + 4452934131562577920e^{\frac{t\omega_b^3}{32}+t\omega_b-\frac{5t}{2\omega_b}}tp_{\omega_b}\omega_b^{15} + 8905868263125155840e^{\frac{t\omega_b^3}{32}+t\omega_b-\frac{5t}{2\omega_b}}p_{\omega_b}\omega_b^{14} \\
& - 110117514488835997696e^{\frac{t\omega_b^3}{32}+t\omega_b-\frac{5t}{2\omega_b}}tp_{\omega_b}\omega_b^{13} - 220235028977671995392e^{\frac{t\omega_b^3}{32}+t\omega_b-\frac{5t}{2\omega_b}}p_{\omega_b}\omega_b^{12} \\
& + 215163975797252816896e^{\frac{t\omega_b^3}{32}+t\omega_b-\frac{5t}{2\omega_b}}tp_{\omega_b}\omega_b^{11} + 430327951594505633792e^{\frac{t\omega_b^3}{32}+t\omega_b-\frac{5t}{2\omega_b}}p_{\omega_b}\omega_b^{10} \\
& + 531785043999908167680e^{\frac{t\omega_b^3}{32}+t\omega_b-\frac{5t}{2\omega_b}}tp_{\omega_b}\omega_b^9 + 1063570087999816335360e^{\frac{t\omega_b^3}{32}+t\omega_b-\frac{5t}{2\omega_b}}p_{\omega_b}\omega_b^8 \\
& - 2854633645406553112576e^{\frac{t\omega_b^3}{32}+t\omega_b-\frac{5t}{2\omega_b}}tp_{\omega_b}\omega_b^7 - 5709267290813106225152e^{\frac{t\omega_b^3}{32}+t\omega_b-\frac{5t}{2\omega_b}}p_{\omega_b}\omega_b^6 \\
& + 4869940435459321626624e^{\frac{t\omega_b^3}{32}+t\omega_b-\frac{5t}{2\omega_b}}tp_{\omega_b}\omega_b^5 + 9739880870918643253248e^{\frac{t\omega_b^3}{32}+t\omega_b-\frac{5t}{2\omega_b}}p_{\omega_b}\omega_b^4 \\
& - 3836922767331586736128e^{\frac{t\omega_b^3}{32}+t\omega_b-\frac{5t}{2\omega_b}}tp_{\omega_b}\omega_b^3 - 7673845534663173472256e^{\frac{t\omega_b^3}{32}+t\omega_b-\frac{5t}{2\omega_b}}p_{\omega_b}\omega_b^2 \\
& + 1180591620717411303424e^{\frac{t\omega_b^3}{32}+t\omega_b-\frac{5t}{2\omega_b}}tp_{\omega_b}\omega_b + 2361183241434822606848e^{\frac{t\omega_b^3}{32}+t\omega_b-\frac{5t}{2\omega_b}}p_{\omega_b},
\end{aligned}$$

where we have used ω_b as defined in Eq. (39), and defined

$$p_{\omega_b} = \sqrt{11\omega_b^4 - \omega_b^6 + 48\omega_b^2 - 56} \quad (C3)$$

for brevity.

Similar to the quark case above, we define the asymptotic gluon OAM to gluon hPDF ratio $R_G(t)$ as

$$R_G(t) = \frac{N_G(t)}{D_G(t)}. \quad (C4)$$

Following the procedure from the main text, one obtains

$$\begin{aligned}
N_G(t) = & 3e^{\frac{1}{32}t\omega_b(\omega_b^2+16)-\frac{5t}{2\omega_b}}p_{\omega_b}\omega_b^{46} + 720e^{\frac{1}{32}t\omega_b(\omega_b^2+16)-\frac{5t}{2\omega_b}}p_{\omega_b}\omega_b^{44} + 51744e^{\frac{1}{32}t\omega_b(\omega_b^2+16)-\frac{5t}{2\omega_b}}p_{\omega_b}\omega_b^{42} \\
& - 2048e^{\frac{t\omega_b^3}{32}+t\omega_b-\frac{5t}{2\omega_b}}tp_{\omega_b}\omega_b^{41} - 4096e^{\frac{t\omega_b^3}{32}+t\omega_b-\frac{5t}{2\omega_b}}p_{\omega_b}\omega_b^{40} + 573696e^{\frac{1}{32}t\omega_b(\omega_b^2+16)-\frac{5t}{2\omega_b}}p_{\omega_b}\omega_b^{40} \\
& - 494080e^{\frac{t\omega_b^3}{32}+t\omega_b-\frac{5t}{2\omega_b}}tp_{\omega_b}\omega_b^{39} - 25165824\sqrt{2}e^{\frac{t(\omega_b^4+48\omega_b^2-4\sqrt{2}p_{\omega_b}+80)}{64\omega_b}-\frac{5t}{2\omega_b}}\omega_b^{38} - 1007616e^{\frac{t\omega_b^3}{32}+t\omega_b-\frac{5t}{2\omega_b}}p_{\omega_b}\omega_b^{38} \\
& - 52880640e^{\frac{1}{32}t\omega_b(\omega_b^2+16)-\frac{5t}{2\omega_b}}p_{\omega_b}\omega_b^{38} + 25165824e^{\frac{t(\omega_b^4+48\omega_b^2+4p_{\omega_b}\sqrt{2}+80)}{64\omega_b}-\frac{5t}{2\omega_b}}\sqrt{2}\omega_b^{38} \\
& - 36444160e^{\frac{t\omega_b^3}{32}+t\omega_b-\frac{5t}{2\omega_b}}tp_{\omega_b}\omega_b^{37} - 767557632\sqrt{2}e^{\frac{t(\omega_b^4+48\omega_b^2-4\sqrt{2}p_{\omega_b}+80)}{64\omega_b}-\frac{5t}{2\omega_b}}\omega_b^{36} \\
& - 77893632e^{\frac{t\omega_b^3}{32}+t\omega_b-\frac{5t}{2\omega_b}}p_{\omega_b}\omega_b^{36} - 2097152e^{\frac{t(\omega_b^4+48\omega_b^2+4p_{\omega_b}\sqrt{2}+80)}{64\omega_b}-\frac{5t}{2\omega_b}}p_{\omega_b}\omega_b^{36} \\
& - 2097152e^{\frac{t(\omega_b^4+48\omega_b^2-4\sqrt{2}p_{\omega_b}+80)}{64\omega_b}-\frac{5t}{2\omega_b}}p_{\omega_b}\omega_b^{36} - 710320128e^{\frac{1}{32}t\omega_b(\omega_b^2+16)-\frac{5t}{2\omega_b}}p_{\omega_b}\omega_b^{36} \\
& + 767557632e^{\frac{t(\omega_b^4+48\omega_b^2+4p_{\omega_b}\sqrt{2}+80)}{64\omega_b}-\frac{5t}{2\omega_b}}\sqrt{2}\omega_b^{36} - 559202304e^{\frac{t\omega_b^3}{32}+t\omega_b-\frac{5t}{2\omega_b}}tp_{\omega_b}\omega_b^{35} \\
& - 3825205248\sqrt{2}e^{\frac{t(\omega_b^4+48\omega_b^2-4\sqrt{2}p_{\omega_b}+80)}{64\omega_b}-\frac{5t}{2\omega_b}}\omega_b^{34} - 1543700480e^{\frac{t\omega_b^3}{32}+t\omega_b-\frac{5t}{2\omega_b}}p_{\omega_b}\omega_b^{34} \\
& + 33554432e^{\frac{t(\omega_b^4+48\omega_b^2+4p_{\omega_b}\sqrt{2}+80)}{64\omega_b}-\frac{5t}{2\omega_b}}p_{\omega_b}\omega_b^{34} + 33554432e^{\frac{t(\omega_b^4+48\omega_b^2-4\sqrt{2}p_{\omega_b}+80)}{64\omega_b}-\frac{5t}{2\omega_b}}p_{\omega_b}\omega_b^{34} \\
& + 24862507008e^{\frac{1}{32}t\omega_b(\omega_b^2+16)-\frac{5t}{2\omega_b}}p_{\omega_b}\omega_b^{34} + 3825205248e^{\frac{t(\omega_b^4+48\omega_b^2+4p_{\omega_b}\sqrt{2}+80)}{64\omega_b}-\frac{5t}{2\omega_b}}\sqrt{2}\omega_b^{34} \\
& + 26303004672e^{\frac{t\omega_b^3}{32}+t\omega_b-\frac{5t}{2\omega_b}}tp_{\omega_b}\omega_b^{33} - 523851792384\sqrt{2}e^{\frac{t(\omega_b^4+48\omega_b^2+4p_{\omega_b}\sqrt{2}+80)}{64\omega_b}-\frac{5t}{2\omega_b}}\omega_b^{32} \\
& + 40762867712e^{\frac{t\omega_b^3}{32}+t\omega_b-\frac{5t}{2\omega_b}}p_{\omega_b}\omega_b^{32} - 738197504e^{\frac{t(\omega_b^4+48\omega_b^2+4p_{\omega_b}\sqrt{2}+80)}{64\omega_b}-\frac{5t}{2\omega_b}}p_{\omega_b}\omega_b^{32} \\
& - 738197504e^{\frac{t(\omega_b^4+48\omega_b^2-4\sqrt{2}p_{\omega_b}+80)}{64\omega_b}-\frac{5t}{2\omega_b}}p_{\omega_b}\omega_b^{32} + 213254406144e^{\frac{1}{32}t\omega_b(\omega_b^2+16)-\frac{5t}{2\omega_b}}p_{\omega_b}\omega_b^{32} \\
& + 523851792384e^{\frac{t(\omega_b^4+48\omega_b^2-4\sqrt{2}p_{\omega_b}+80)}{64\omega_b}-\frac{5t}{2\omega_b}}\sqrt{2}\omega_b^{32} + 373427273728e^{\frac{t\omega_b^3}{32}+t\omega_b-\frac{5t}{2\omega_b}}tp_{\omega_b}\omega_b^{31}
\end{aligned} \quad (C5a)$$

$$\begin{aligned}
& -5399847632896\sqrt{2}e^{\frac{t(\omega_b^4+48\omega_b^2+4p\omega_b\sqrt{2}+80)}{64\omega_b}-\frac{5t}{2\omega_b}}\omega_b^{30}+831344607232e^{\frac{t\omega_b^3}{32}+t\omega_b-\frac{5t}{2\omega_b}}p_{\omega_b}\omega_b^{30} \\
& -27380416512e^{\frac{t(\omega_b^4+48\omega_b^2+4p\omega_b\sqrt{2}+80)}{64\omega_b}-\frac{5t}{2\omega_b}}p_{\omega_b}\omega_b^{30}-27380416512e^{\frac{t(\omega_b^4+48\omega_b^2-4\sqrt{2}p\omega_b+80)}{64\omega_b}-\frac{5t}{2\omega_b}}p_{\omega_b}\omega_b^{30} \\
& -6494217043968e^{\frac{1}{32}t\omega_b(\omega_b^2+16)-\frac{5t}{2\omega_b}}p_{\omega_b}\omega_b^{30}+5399847632896e^{\frac{t(\omega_b^4+48\omega_b^2-4\sqrt{2}p\omega_b+80)}{64\omega_b}-\frac{5t}{2\omega_b}}\sqrt{2}\omega_b^{30} \\
& -9810711937024e^{\frac{t\omega_b^3}{32}+t\omega_b-\frac{5t}{2\omega_b}}tp_{\omega_b}\omega_b^{29}-151795955400704\sqrt{2}e^{\frac{t(\omega_b^4+48\omega_b^2-4\sqrt{2}p\omega_b+80)}{64\omega_b}-\frac{5t}{2\omega_b}}\omega_b^{28} \\
& -14009780666368e^{\frac{t\omega_b^3}{32}+t\omega_b-\frac{5t}{2\omega_b}}p_{\omega_b}\omega_b^{28}+2406792298496e^{\frac{t(\omega_b^4+48\omega_b^2+4p\omega_b\sqrt{2}+80)}{64\omega_b}-\frac{5t}{2\omega_b}}p_{\omega_b}\omega_b^{28} \\
& +2406792298496e^{\frac{t(\omega_b^4+48\omega_b^2-4\sqrt{2}p\omega_b+80)}{64\omega_b}-\frac{5t}{2\omega_b}}p_{\omega_b}\omega_b^{28}-21791590318080e^{\frac{1}{32}t\omega_b(\omega_b^2+16)-\frac{5t}{2\omega_b}}p_{\omega_b}\omega_b^{28} \\
& +151795955400704e^{\frac{t(\omega_b^4+48\omega_b^2+4p\omega_b\sqrt{2}+80)}{64\omega_b}-\frac{5t}{2\omega_b}}\sqrt{2}\omega_b^{28}-50353122836480e^{\frac{t\omega_b^3}{32}+t\omega_b-\frac{5t}{2\omega_b}}tp_{\omega_b}\omega_b^{27} \\
& -741861111103488\sqrt{2}e^{\frac{t(\omega_b^4+48\omega_b^2-4\sqrt{2}p\omega_b+80)}{64\omega_b}-\frac{5t}{2\omega_b}}\omega_b^{26}-107827301449728e^{\frac{t\omega_b^3}{32}+t\omega_b-\frac{5t}{2\omega_b}}p_{\omega_b}\omega_b^{26} \\
& +4140348473344e^{\frac{t(\omega_b^4+48\omega_b^2+4p\omega_b\sqrt{2}+80)}{64\omega_b}-\frac{5t}{2\omega_b}}p_{\omega_b}\omega_b^{26}+4140348473344e^{\frac{t(\omega_b^4+48\omega_b^2-4\sqrt{2}p\omega_b+80)}{64\omega_b}-\frac{5t}{2\omega_b}}p_{\omega_b}\omega_b^{26} \\
& +934671588261888e^{\frac{1}{32}t\omega_b(\omega_b^2+16)-\frac{5t}{2\omega_b}}p_{\omega_b}\omega_b^{26}+741861111103488e^{\frac{t(\omega_b^4+48\omega_b^2+4p\omega_b\sqrt{2}+80)}{64\omega_b}-\frac{5t}{2\omega_b}}\sqrt{2}\omega_b^{26} \\
& +1752851315425280e^{\frac{t\omega_b^3}{32}+t\omega_b-\frac{5t}{2\omega_b}}tp_{\omega_b}\omega_b^{25}-17967050790010880\sqrt{2}e^{\frac{t(\omega_b^4+48\omega_b^2+4p\omega_b\sqrt{2}+80)}{64\omega_b}-\frac{5t}{2\omega_b}}\omega_b^{24} \\
& +2561436890955776e^{\frac{t\omega_b^3}{32}+t\omega_b-\frac{5t}{2\omega_b}}p_{\omega_b}\omega_b^{24}-764882135810048e^{\frac{t(\omega_b^4+48\omega_b^2+4p\omega_b\sqrt{2}+80)}{64\omega_b}-\frac{5t}{2\omega_b}}p_{\omega_b}\omega_b^{24} \\
& -764882135810048e^{\frac{t(\omega_b^4+48\omega_b^2-4\sqrt{2}p\omega_b+80)}{64\omega_b}-\frac{5t}{2\omega_b}}p_{\omega_b}\omega_b^{24}-301558243786752e^{\frac{1}{32}t\omega_b(\omega_b^2+16)-\frac{5t}{2\omega_b}}p_{\omega_b}\omega_b^{24} \\
& +17967050790010880e^{\frac{t(\omega_b^4+48\omega_b^2-4\sqrt{2}p\omega_b+80)}{64\omega_b}-\frac{5t}{2\omega_b}}\sqrt{2}\omega_b^{24}-3616723240484864e^{\frac{t\omega_b^3}{32}+t\omega_b-\frac{5t}{2\omega_b}}tp_{\omega_b}\omega_b^{23} \\
& -27413023903711232\sqrt{2}e^{\frac{t(\omega_b^4+48\omega_b^2+4p\omega_b\sqrt{2}+80)}{64\omega_b}-\frac{5t}{2\omega_b}}\omega_b^{22}-5950350771093504e^{\frac{t\omega_b^3}{32}+t\omega_b-\frac{5t}{2\omega_b}}p_{\omega_b}\omega_b^{22} \\
& +1801000046297088e^{\frac{t(\omega_b^4+48\omega_b^2+4p\omega_b\sqrt{2}+80)}{64\omega_b}-\frac{5t}{2\omega_b}}p_{\omega_b}\omega_b^{22}+1801000046297088e^{\frac{t(\omega_b^4+48\omega_b^2-4\sqrt{2}p\omega_b+80)}{64\omega_b}-\frac{5t}{2\omega_b}}p_{\omega_b}\omega_b^{22} \\
& -72638222076739584e^{\frac{1}{32}t\omega_b(\omega_b^2+16)-\frac{5t}{2\omega_b}}p_{\omega_b}\omega_b^{22}+27413023903711232e^{\frac{t(\omega_b^4+48\omega_b^2-4\sqrt{2}p\omega_b+80)}{64\omega_b}-\frac{5t}{2\omega_b}}\sqrt{2}\omega_b^{22} \\
& -97407659250024448e^{\frac{t\omega_b^3}{32}+t\omega_b-\frac{5t}{2\omega_b}}tp_{\omega_b}\omega_b^{21}-817908008204894208\sqrt{2}e^{\frac{t(\omega_b^4+48\omega_b^2+4p\omega_b\sqrt{2}+80)}{64\omega_b}-\frac{5t}{2\omega_b}}\omega_b^{20} \\
& -140594551843717120e^{\frac{t\omega_b^3}{32}+t\omega_b-\frac{5t}{2\omega_b}}p_{\omega_b}\omega_b^{20}+85902094699069440e^{\frac{t(\omega_b^4+48\omega_b^2+4p\omega_b\sqrt{2}+80)}{64\omega_b}-\frac{5t}{2\omega_b}}p_{\omega_b}\omega_b^{20} \\
& +85902094699069440e^{\frac{t(\omega_b^4+48\omega_b^2-4\sqrt{2}p\omega_b+80)}{64\omega_b}-\frac{5t}{2\omega_b}}p_{\omega_b}\omega_b^{20}+210661754957463552e^{\frac{1}{32}t\omega_b(\omega_b^2+16)-\frac{5t}{2\omega_b}}p_{\omega_b}\omega_b^{20} \\
& +817908008204894208e^{\frac{t(\omega_b^4+48\omega_b^2+4p\omega_b\sqrt{2}+80)}{64\omega_b}-\frac{5t}{2\omega_b}}\sqrt{2}\omega_b^{20}+621934354204983296e^{\frac{t\omega_b^3}{32}+t\omega_b-\frac{5t}{2\omega_b}}tp_{\omega_b}\omega_b^{19} \\
& -811421989112643584\sqrt{2}e^{\frac{t(\omega_b^4+48\omega_b^2-4\sqrt{2}p\omega_b+80)}{64\omega_b}-\frac{5t}{2\omega_b}}\omega_b^{18}+1225955464970240000e^{\frac{t\omega_b^3}{32}+t\omega_b-\frac{5t}{2\omega_b}}p_{\omega_b}\omega_b^{18} \\
& -404796200882012160e^{\frac{t(\omega_b^4+48\omega_b^2+4p\omega_b\sqrt{2}+80)}{64\omega_b}-\frac{5t}{2\omega_b}}p_{\omega_b}\omega_b^{18}-404796200882012160e^{\frac{t(\omega_b^4+48\omega_b^2-4\sqrt{2}p\omega_b+80)}{64\omega_b}-\frac{5t}{2\omega_b}}p_{\omega_b}\omega_b^{18} \\
& +2786186654040195072e^{\frac{1}{32}t\omega_b(\omega_b^2+16)-\frac{5t}{2\omega_b}}p_{\omega_b}\omega_b^{18}+811421989112643584e^{\frac{t(\omega_b^4+48\omega_b^2+4p\omega_b\sqrt{2}+80)}{64\omega_b}-\frac{5t}{2\omega_b}}\sqrt{2}\omega_b^{18} \\
& -352230748981297152e^{\frac{t\omega_b^3}{32}+t\omega_b-\frac{5t}{2\omega_b}}tp_{\omega_b}\omega_b^{17}-11789614583897915392\sqrt{2}e^{\frac{t(\omega_b^4+48\omega_b^2+4p\omega_b\sqrt{2}+80)}{64\omega_b}-\frac{5t}{2\omega_b}}\omega_b^{16} \\
& -1120551882285121536e^{\frac{t\omega_b^3}{32}+t\omega_b-\frac{5t}{2\omega_b}}p_{\omega_b}\omega_b^{16}-3398089064153350144e^{\frac{t(\omega_b^4+48\omega_b^2+4p\omega_b\sqrt{2}+80)}{64\omega_b}-\frac{5t}{2\omega_b}}p_{\omega_b}\omega_b^{16} \\
& -3398089064153350144e^{\frac{t(\omega_b^4+48\omega_b^2-4\sqrt{2}p\omega_b+80)}{64\omega_b}-\frac{5t}{2\omega_b}}p_{\omega_b}\omega_b^{16}-14601690338725724160e^{\frac{1}{32}t\omega_b(\omega_b^2+16)-\frac{5t}{2\omega_b}}p_{\omega_b}\omega_b^{16}
\end{aligned}$$

$$\begin{aligned}
& + 11789614583897915392e^{\frac{t(\omega_b^4+48\omega_b^2-4\sqrt{2}p\omega_b+80)}{64\omega_b}-\frac{5t}{2\omega_b}}\sqrt{2}\omega_b^{16} - 13657447344977739776e^{\frac{t\omega_b^3}{32}+t\omega_b-\frac{5t}{2\omega_b}}tp_{\omega_b}\omega_b^{15} \\
& - 84602933749921873920\sqrt{2}e^{\frac{t(\omega_b^4+48\omega_b^2+4p\omega_b\sqrt{2}+80)}{64\omega_b}-\frac{5t}{2\omega_b}}\omega_b^{14} - 36435246885334155264e^{\frac{t\omega_b^3}{32}+t\omega_b-\frac{5t}{2\omega_b}}p_{\omega_b}\omega_b^{14} \\
& + 24123812878986772480e^{\frac{t(\omega_b^4+48\omega_b^2+4p\omega_b\sqrt{2}+80)}{64\omega_b}-\frac{5t}{2\omega_b}}p_{\omega_b}\omega_b^{14} + 24123812878986772480e^{\frac{t(\omega_b^4+48\omega_b^2-4\sqrt{2}p\omega_b+80)}{64\omega_b}-\frac{5t}{2\omega_b}}p_{\omega_b}\omega_b^{14} \\
& - 34005836361344483328e^{\frac{1}{32}t\omega_b(\omega_b^2+16)-\frac{5t}{2\omega_b}}p_{\omega_b}\omega_b^{14} + 84602933749921873920e^{\frac{t(\omega_b^4+48\omega_b^2-4\sqrt{2}p\omega_b+80)}{64\omega_b}-\frac{5t}{2\omega_b}}\sqrt{2}\omega_b^{14} \\
& + 114882322894593982464e^{\frac{t\omega_b^3}{32}+t\omega_b-\frac{5t}{2\omega_b}}tp_{\omega_b}\omega_b^{13} - 309548164987869986816\sqrt{2}e^{\frac{t(\omega_b^4+48\omega_b^2-4\sqrt{2}p\omega_b+80)}{64\omega_b}-\frac{5t}{2\omega_b}}\omega_b^{12} \\
& + 204931797443867049984e^{\frac{t\omega_b^3}{32}+t\omega_b-\frac{5t}{2\omega_b}}p_{\omega_b}\omega_b^{12} + 6423258968537169920e^{\frac{t(\omega_b^4+48\omega_b^2+4p\omega_b\sqrt{2}+80)}{64\omega_b}-\frac{5t}{2\omega_b}}p_{\omega_b}\omega_b^{12} \\
& + 6423258968537169920e^{\frac{t(\omega_b^4+48\omega_b^2-4\sqrt{2}p\omega_b+80)}{64\omega_b}-\frac{5t}{2\omega_b}}p_{\omega_b}\omega_b^{12} + 370695788928492896256e^{\frac{1}{32}t\omega_b(\omega_b^2+16)-\frac{5t}{2\omega_b}}p_{\omega_b}\omega_b^{12} \\
& + 309548164987869986816e^{\frac{t(\omega_b^4+48\omega_b^2+4p\omega_b\sqrt{2}+80)}{64\omega_b}-\frac{5t}{2\omega_b}}\sqrt{2}\omega_b^{12} - 359423279061184544768e^{\frac{t\omega_b^3}{32}+t\omega_b-\frac{5t}{2\omega_b}}tp_{\omega_b}\omega_b^{11} \\
& - 868402094548088520704\sqrt{2}e^{\frac{t(\omega_b^4+48\omega_b^2-4\sqrt{2}p\omega_b+80)}{64\omega_b}-\frac{5t}{2\omega_b}}\omega_b^{10} - 267333673880712642560e^{\frac{t\omega_b^3}{32}+t\omega_b-\frac{5t}{2\omega_b}}p_{\omega_b}\omega_b^{10} \\
& - 325394080276773076992e^{\frac{t(\omega_b^4+48\omega_b^2+4p\omega_b\sqrt{2}+80)}{64\omega_b}-\frac{5t}{2\omega_b}}p_{\omega_b}\omega_b^{10} - 325394080276773076992e^{\frac{t(\omega_b^4+48\omega_b^2-4\sqrt{2}p\omega_b+80)}{64\omega_b}-\frac{5t}{2\omega_b}}p_{\omega_b}\omega_b^{10} \\
& - 545782231641775669248e^{\frac{1}{32}t\omega_b(\omega_b^2+16)-\frac{5t}{2\omega_b}}p_{\omega_b}\omega_b^{10} + 868402094548088520704e^{\frac{t(\omega_b^4+48\omega_b^2+4p\omega_b\sqrt{2}+80)}{64\omega_b}-\frac{5t}{2\omega_b}}\sqrt{2}\omega_b^{10} \\
& - 504547273453571407872e^{\frac{t\omega_b^3}{32}+t\omega_b-\frac{5t}{2\omega_b}}tp_{\omega_b}\omega_b^9 - 4440188944617119416320\sqrt{2}e^{\frac{t(\omega_b^4+48\omega_b^2+4p\omega_b\sqrt{2}+80)}{64\omega_b}-\frac{5t}{2\omega_b}}\omega_b^8 \\
& - 1566532094384553328640e^{\frac{t\omega_b^3}{32}+t\omega_b-\frac{5t}{2\omega_b}}p_{\omega_b}\omega_b^8 + 772601523274663329792e^{\frac{t(\omega_b^4+48\omega_b^2+4p\omega_b\sqrt{2}+80)}{64\omega_b}-\frac{5t}{2\omega_b}}p_{\omega_b}\omega_b^8 \\
& + 772601523274663329792e^{\frac{t(\omega_b^4+48\omega_b^2-4\sqrt{2}p\omega_b+80)}{64\omega_b}-\frac{5t}{2\omega_b}}p_{\omega_b}\omega_b^8 - 2130598940513453211648e^{\frac{1}{32}t\omega_b(\omega_b^2+16)-\frac{5t}{2\omega_b}}p_{\omega_b}\omega_b^8 \\
& + 4440188944617119416320e^{\frac{t(\omega_b^4+48\omega_b^2-4\sqrt{2}p\omega_b+80)}{64\omega_b}-\frac{5t}{2\omega_b}}\sqrt{2}\omega_b^8 + 6245375790455290068992e^{\frac{t\omega_b^3}{32}+t\omega_b-\frac{5t}{2\omega_b}}tp_{\omega_b}\omega_b^7 \\
& - 5688514703730182979584\sqrt{2}e^{\frac{t(\omega_b^4+48\omega_b^2-4\sqrt{2}p\omega_b+80)}{64\omega_b}-\frac{5t}{2\omega_b}}\omega_b^6 + 8388656867519418597376e^{\frac{t\omega_b^3}{32}+t\omega_b-\frac{5t}{2\omega_b}}p_{\omega_b}\omega_b^6 \\
& - 616813004964663132160e^{\frac{t(\omega_b^4+48\omega_b^2+4p\omega_b\sqrt{2}+80)}{64\omega_b}-\frac{5t}{2\omega_b}}p_{\omega_b}\omega_b^6 - 616813004964663132160e^{\frac{t(\omega_b^4+48\omega_b^2-4\sqrt{2}p\omega_b+80)}{64\omega_b}-\frac{5t}{2\omega_b}}p_{\omega_b}\omega_b^6 \\
& + 9477014767868282142720e^{\frac{1}{32}t\omega_b(\omega_b^2+16)-\frac{5t}{2\omega_b}}p_{\omega_b}\omega_b^6 + 5688514703730182979584e^{\frac{t(\omega_b^4+48\omega_b^2+4p\omega_b\sqrt{2}+80)}{64\omega_b}-\frac{5t}{2\omega_b}}\sqrt{2}\omega_b^6 \\
& - 16002550483943036026880e^{\frac{t\omega_b^3}{32}+t\omega_b-\frac{5t}{2\omega_b}}tp_{\omega_b}\omega_b^5 - 2287396265139984400384\sqrt{2}e^{\frac{t(\omega_b^4+48\omega_b^2+4p\omega_b\sqrt{2}+80)}{64\omega_b}-\frac{5t}{2\omega_b}}\omega_b^4 \\
& - 17764214542982298206208e^{\frac{t\omega_b^3}{32}+t\omega_b-\frac{5t}{2\omega_b}}p_{\omega_b}\omega_b^4 + 110680464442257309696e^{\frac{t(\omega_b^4+48\omega_b^2+4p\omega_b\sqrt{2}+80)}{64\omega_b}-\frac{5t}{2\omega_b}}p_{\omega_b}\omega_b^4 \\
& + 110680464442257309696e^{\frac{t(\omega_b^4+48\omega_b^2-4\sqrt{2}p\omega_b+80)}{64\omega_b}-\frac{5t}{2\omega_b}}p_{\omega_b}\omega_b^4 - 15329244325252637392896e^{\frac{1}{32}t\omega_b(\omega_b^2+16)-\frac{5t}{2\omega_b}}p_{\omega_b}\omega_b^4 \\
& + 2287396265139984400384e^{\frac{t(\omega_b^4+48\omega_b^2-4\sqrt{2}p\omega_b+80)}{64\omega_b}-\frac{5t}{2\omega_b}}\sqrt{2}\omega_b^4 + 17487513381876654931968e^{\frac{t\omega_b^3}{32}+t\omega_b-\frac{5t}{2\omega_b}}tp_{\omega_b}\omega_b^3 \\
& + 18004022215940522377216e^{\frac{t\omega_b^3}{32}+t\omega_b-\frac{5t}{2\omega_b}}p_{\omega_b}\omega_b^2 + 11732129230879274827776e^{\frac{1}{32}t\omega_b(\omega_b^2+16)-\frac{5t}{2\omega_b}}p_{\omega_b}\omega_b^2 \\
& - 7083549724304467820544e^{\frac{t\omega_b^3}{32}+t\omega_b-\frac{5t}{2\omega_b}}tp_{\omega_b}\omega_b - 7083549724304467820544e^{\frac{t\omega_b^3}{32}+t\omega_b-\frac{5t}{2\omega_b}}p_{\omega_b} \\
& - 3541774862152233910272e^{\frac{1}{32}t\omega_b(\omega_b^2+16)-\frac{5t}{2\omega_b}}p_{\omega_b}, \\
D_G(t) = & 16e^{\frac{t\omega_b^3}{32}+t\omega_b-\frac{5t}{2\omega_b}}tp_{\omega_b}\omega_b^{45} + 32e^{\frac{t\omega_b^3}{32}+t\omega_b-\frac{5t}{2\omega_b}}p_{\omega_b}\omega_b^{44} + 4096e^{\frac{t\omega_b^3}{32}+t\omega_b-\frac{5t}{2\omega_b}}tp_{\omega_b}\omega_b^{43} + 8192e^{\frac{t\omega_b^3}{32}+t\omega_b-\frac{5t}{2\omega_b}}p_{\omega_b}\omega_b^{42} \\
& + 341504e^{\frac{t\omega_b^3}{32}+t\omega_b-\frac{5t}{2\omega_b}}tp_{\omega_b}\omega_b^{41} + 683008e^{\frac{t\omega_b^3}{32}+t\omega_b-\frac{5t}{2\omega_b}}p_{\omega_b}\omega_b^{40} + 8523776e^{\frac{t\omega_b^3}{32}+t\omega_b-\frac{5t}{2\omega_b}}tp_{\omega_b}\omega_b^{39} \\
& + 17047552e^{\frac{t\omega_b^3}{32}+t\omega_b-\frac{5t}{2\omega_b}}p_{\omega_b}\omega_b^{38} - 145649664e^{\frac{t\omega_b^3}{32}+t\omega_b-\frac{5t}{2\omega_b}}tp_{\omega_b}\omega_b^{37} - 291299328e^{\frac{t\omega_b^3}{32}+t\omega_b-\frac{5t}{2\omega_b}}p_{\omega_b}\omega_b^{36}
\end{aligned}
\tag{C5b}$$

$$\begin{aligned}
& -6118768640e^{\frac{t\omega_b^3}{32}+t\omega_b-\frac{5t}{2\omega_b}}tp_{\omega_b}\omega_b^{35} - 12237537280e^{\frac{t\omega_b^3}{32}+t\omega_b-\frac{5t}{2\omega_b}}p_{\omega_b}\omega_b^{34} + 34699739136e^{\frac{t\omega_b^3}{32}+t\omega_b-\frac{5t}{2\omega_b}}tp_{\omega_b}\omega_b^{33} \\
& + 69399478272e^{\frac{t\omega_b^3}{32}+t\omega_b-\frac{5t}{2\omega_b}}p_{\omega_b}\omega_b^{32} + 1692552658944e^{\frac{t\omega_b^3}{32}+t\omega_b-\frac{5t}{2\omega_b}}tp_{\omega_b}\omega_b^{31} + 3385105317888e^{\frac{t\omega_b^3}{32}+t\omega_b-\frac{5t}{2\omega_b}}p_{\omega_b}\omega_b^{30} \\
& - 7554981691392e^{\frac{t\omega_b^3}{32}+t\omega_b-\frac{5t}{2\omega_b}}tp_{\omega_b}\omega_b^{29} - 15109963382784e^{\frac{t\omega_b^3}{32}+t\omega_b-\frac{5t}{2\omega_b}}p_{\omega_b}\omega_b^{28} \\
& - 237101522092032e^{\frac{t\omega_b^3}{32}+t\omega_b-\frac{5t}{2\omega_b}}tp_{\omega_b}\omega_b^{27} - 474203044184064e^{\frac{t\omega_b^3}{32}+t\omega_b-\frac{5t}{2\omega_b}}p_{\omega_b}\omega_b^{26} \\
& + 1191290783924224e^{\frac{t\omega_b^3}{32}+t\omega_b-\frac{5t}{2\omega_b}}tp_{\omega_b}\omega_b^{25} + 2382581567848448e^{\frac{t\omega_b^3}{32}+t\omega_b-\frac{5t}{2\omega_b}}p_{\omega_b}\omega_b^{24} \\
& + 17452341909258240e^{\frac{t\omega_b^3}{32}+t\omega_b-\frac{5t}{2\omega_b}}tp_{\omega_b}\omega_b^{23} + 34904683818516480e^{\frac{t\omega_b^3}{32}+t\omega_b-\frac{5t}{2\omega_b}}p_{\omega_b}\omega_b^{22} \\
& - 108166380527812608e^{\frac{t\omega_b^3}{32}+t\omega_b-\frac{5t}{2\omega_b}}tp_{\omega_b}\omega_b^{21} - 216332761055625216e^{\frac{t\omega_b^3}{32}+t\omega_b-\frac{5t}{2\omega_b}}p_{\omega_b}\omega_b^{20} \\
& - 607132728671862784e^{\frac{t\omega_b^3}{32}+t\omega_b-\frac{5t}{2\omega_b}}tp_{\omega_b}\omega_b^{19} - 1214265457343725568e^{\frac{t\omega_b^3}{32}+t\omega_b-\frac{5t}{2\omega_b}}p_{\omega_b}\omega_b^{18} \\
& + 5145538496131235840e^{\frac{t\omega_b^3}{32}+t\omega_b-\frac{5t}{2\omega_b}}tp_{\omega_b}\omega_b^{17} + 10291076992262471680e^{\frac{t\omega_b^3}{32}+t\omega_b-\frac{5t}{2\omega_b}}p_{\omega_b}\omega_b^{16} \\
& + 4452934131562577920e^{\frac{t\omega_b^3}{32}+t\omega_b-\frac{5t}{2\omega_b}}tp_{\omega_b}\omega_b^{15} + 8905868263125155840e^{\frac{t\omega_b^3}{32}+t\omega_b-\frac{5t}{2\omega_b}}p_{\omega_b}\omega_b^{14} \\
& - 110117514488835997696e^{\frac{t\omega_b^3}{32}+t\omega_b-\frac{5t}{2\omega_b}}tp_{\omega_b}\omega_b^{13} - 220235028977671995392e^{\frac{t\omega_b^3}{32}+t\omega_b-\frac{5t}{2\omega_b}}p_{\omega_b}\omega_b^{12} \\
& + 215163975797252816896e^{\frac{t\omega_b^3}{32}+t\omega_b-\frac{5t}{2\omega_b}}tp_{\omega_b}\omega_b^{11} + 430327951594505633792e^{\frac{t\omega_b^3}{32}+t\omega_b-\frac{5t}{2\omega_b}}p_{\omega_b}\omega_b^{10} \\
& + 531785043999908167680e^{\frac{t\omega_b^3}{32}+t\omega_b-\frac{5t}{2\omega_b}}tp_{\omega_b}\omega_b^9 + 1063570087999816335360e^{\frac{t\omega_b^3}{32}+t\omega_b-\frac{5t}{2\omega_b}}p_{\omega_b}\omega_b^8 \\
& - 2854633645406553112576e^{\frac{t\omega_b^3}{32}+t\omega_b-\frac{5t}{2\omega_b}}tp_{\omega_b}\omega_b^7 - 5709267290813106225152e^{\frac{t\omega_b^3}{32}+t\omega_b-\frac{5t}{2\omega_b}}p_{\omega_b}\omega_b^6 \\
& + 4869940435459321626624e^{\frac{t\omega_b^3}{32}+t\omega_b-\frac{5t}{2\omega_b}}tp_{\omega_b}\omega_b^5 + 9739880870918643253248e^{\frac{t\omega_b^3}{32}+t\omega_b-\frac{5t}{2\omega_b}}p_{\omega_b}\omega_b^4 \\
& - 3836922767331586736128e^{\frac{t\omega_b^3}{32}+t\omega_b-\frac{5t}{2\omega_b}}tp_{\omega_b}\omega_b^3 - 7673845534663173472256e^{\frac{t\omega_b^3}{32}+t\omega_b-\frac{5t}{2\omega_b}}p_{\omega_b}\omega_b^2 \\
& + 1180591620717411303424e^{\frac{t\omega_b^3}{32}+t\omega_b-\frac{5t}{2\omega_b}}tp_{\omega_b}\omega_b + 2361183241434822606848e^{\frac{t\omega_b^3}{32}+t\omega_b-\frac{5t}{2\omega_b}}p_{\omega_b}.
\end{aligned}$$

-
- [1] Y.V. Kovchegov and B. Manley, *Orbital Angular Momentum at Small x Revisited*, 2310.18404.
 - [2] Y.V. Kovchegov, *Orbital Angular Momentum at Small x*, *JHEP* **03** (2019) 174 [1901.07453].
 - [3] J. Borden and Y.V. Kovchegov, *Analytic solution for the revised helicity evolution at small x and large Nc: New resummed gluon-gluon polarized anomalous dimension and intercept*, *Phys. Rev. D* **108** (2023) 014001 [2304.06161].
 - [4] R. Boussarie, Y. Hatta and F. Yuan, *Proton Spin Structure at Small-x*, *Phys. Lett.* **B797** (2019) 134817 [1904.02693].
 - [5] C.A. Aidala, S.D. Bass, D. Hasch and G.K. Mallot, *The Spin Structure of the Nucleon*, *Rev. Mod. Phys.* **85** (2013) 655 [1209.2803].
 - [6] A. Accardi et al., *Electron Ion Collider: The Next QCD Frontier*, *Eur. Phys. J.* **A52** (2016) 268 [1212.1701].
 - [7] E. Leader and C. Lorcé, *The angular momentum controversy: What's it all about and does it matter?*, *Phys. Rept.* **541** (2014) 163 [1309.4235].
 - [8] E.C. Aschenauer et al., *The RHIC Spin Program: Achievements and Future Opportunities*, 1304.0079.
 - [9] E.-C. Aschenauer et al., *The RHIC SPIN Program: Achievements and Future Opportunities*, 1501.01220.
 - [10] D. Boer et al., *Gluons and the quark sea at high energies: Distributions, polarization, tomography*, 1108.1713.
 - [11] A. Prokudin, Y. Hatta, Y. Kovchegov and C. Marquet, eds., *Proceedings, Probing Nucleons and Nuclei in High Energy Collisions: Dedicated to the Physics of the Electron Ion Collider: Seattle (WA), United States, October 1 - November 16, 2018*, WSP, 2020. 10.1142/11684.
 - [12] X. Ji, F. Yuan and Y. Zhao, *What we know and what we don't know about the proton spin after 30 years*, *Nature Rev. Phys.* **3** (2021) 27 [2009.01291].
 - [13] R. Abdul Khalek et al., *Science Requirements and Detector Concepts for the Electron-Ion Collider: EIC Yellow Report*, 2103.05419.
 - [14] X.-D. Ji, *Gauge-Invariant Decomposition of Nucleon Spin*, *Phys. Rev. Lett.* **78** (1997) 610 [hep-ph/9603249].
 - [15] R.L. Jaffe and A. Manohar, *The G(1) Problem: Fact and Fantasy on the Spin of the Proton*, *Nucl. Phys.* **B337** (1990) 509.
 - [16] S. Bashinsky and R.L. Jaffe, *Quark and gluon orbital angular momentum and spin in hard processes*, *Nucl. Phys.* **B536**

- (1998) 303 [[hep-ph/9804397](#)].
- [17] P. Hagler and A. Schafer, *Evolution equations for higher moments of angular momentum distributions*, *Phys. Lett.* **B430** (1998) 179 [[hep-ph/9802362](#)].
- [18] A. Harindranath and R. Kundu, *On Orbital angular momentum in deep inelastic scattering*, *Phys. Rev.* **D59** (1999) 116013 [[hep-ph/9802406](#)].
- [19] Y. Hatta and S. Yoshida, *Twist analysis of the nucleon spin in QCD*, *JHEP* **10** (2012) 080 [[1207.5332](#)].
- [20] X. Ji, X. Xiong and F. Yuan, *Probing Parton Orbital Angular Momentum in Longitudinally Polarized Nucleon*, *Phys. Rev.* **D88** (2013) 014041 [[1207.5221](#)].
- [21] M. Gluck, E. Reya, M. Stratmann and W. Vogelsang, *Models for the polarized parton distributions of the nucleon*, *Phys. Rev. D* **63** (2001) 094005 [[hep-ph/0011215](#)].
- [22] E. Leader, A.V. Sidorov and D.B. Stamenov, *Longitudinal polarized parton densities updated*, *Phys. Rev.* **D73** (2006) 034023 [[hep-ph/0512114](#)].
- [23] D. de Florian, R. Sassot, M. Stratmann and W. Vogelsang, *Extraction of Spin-Dependent Parton Densities and Their Uncertainties*, *Phys. Rev.* **D80** (2009) 034030 [[0904.3821](#)].
- [24] E. Leader, A.V. Sidorov and D.B. Stamenov, *Determination of Polarized PDFs from a QCD Analysis of Inclusive and Semi-inclusive Deep Inelastic Scattering Data*, *Phys. Rev.* **D82** (2010) 114018 [[1010.0574](#)].
- [25] P. Jimenez-Delgado, A. Accardi and W. Melnitchouk, *Impact of hadronic and nuclear corrections on global analysis of spin-dependent parton distributions*, *Phys. Rev.* **D89** (2014) 034025 [[1310.3734](#)].
- [26] NNPDF collaboration, *Unbiased determination of polarized parton distributions and their uncertainties*, *Nucl. Phys.* **B874** (2013) 36 [[1303.7236](#)].
- [27] NNPDF collaboration, *A first unbiased global determination of polarized PDFs and their uncertainties*, *Nucl. Phys.* **B887** (2014) 276 [[1406.5539](#)].
- [28] D. de Florian, R. Sassot, M. Stratmann and W. Vogelsang, *Evidence for polarization of gluons in the proton*, *Phys. Rev. Lett.* **113** (2014) 012001 [[1404.4293](#)].
- [29] E. Leader, A.V. Sidorov and D.B. Stamenov, *New analysis concerning the strange quark polarization puzzle*, *Phys. Rev.* **D91** (2015) 054017 [[1410.1657](#)].
- [30] JEFFERSON LAB ANGULAR MOMENTUM collaboration, *Iterative Monte Carlo analysis of spin-dependent parton distributions*, *Phys. Rev.* **D93** (2016) 074005 [[1601.07782](#)].
- [31] J. Ethier, N. Sato and W. Melnitchouk, *First simultaneous extraction of spin-dependent parton distributions and fragmentation functions from a global QCD analysis*, *Phys. Rev. Lett.* **119** (2017) 132001 [[1705.05889](#)].
- [32] D. De Florian, G.A. Lucero, R. Sassot, M. Stratmann and W. Vogelsang, *Monte Carlo sampling variant of the DSSV14 set of helicity parton densities*, *Phys. Rev. D* **100** (2019) 114027 [[1902.10548](#)].
- [33] I. Borsa, G. Lucero, R. Sassot, E.C. Aschenauer and A.S. Nunes, *Revisiting helicity parton distributions at a future electron-ion collider*, *Phys. Rev. D* **102** (2020) 094018 [[2007.08300](#)].
- [34] JAM COLLABORATION collaboration, *How well do we know the gluon polarization in the proton?*, *Phys. Rev. D* **105** (2022) 074022 [[2201.02075](#)].
- [35] JAM COLLABORATION collaboration, *Polarized antimatter in the proton from a global QCD analysis*, *Phys. Rev. D* **106** (2022) L031502 [[2202.03372](#)].
- [36] P. Hoodbhoy, X.-D. Ji and W. Lu, *Quark orbital - angular - momentum distribution in the nucleon*, *Phys. Rev. D* **59** (1999) 014013 [[hep-ph/9804337](#)].
- [37] S. Bhattacharya, R. Boussarie and Y. Hatta, *Signature of the Gluon Orbital Angular Momentum*, *Phys. Rev. Lett.* **128** (2022) 182002 [[2201.08709](#)].
- [38] S. Bhattacharya, D. Zheng and J. Zhou, *Probing quark orbital angular momentum at EIC and EicC*, **2312.01309**.
- [39] J. Bartels, B. Ermolaev and M. Ryskin, *Nonsinglet contributions to the structure function g_1 at small x* , *Z.Phys.* **C70** (1996) 273 [[hep-ph/9507271](#)].
- [40] J. Bartels, B. Ermolaev and M. Ryskin, *Flavor singlet contribution to the structure function $G(1)$ at small x* , *Z.Phys.* **C72** (1996) 627 [[hep-ph/9603204](#)].
- [41] V.G. Gorshkov, V.N. Gribov, L.N. Lipatov and G.V. Frolov, *Doubly logarithmic asymptotic behavior in quantum electrodynamics*, *Sov. J. Nucl. Phys.* **6** (1968) 95.
- [42] R. Kirschner and L. Lipatov, *Double Logarithmic Asymptotics and Regge Singularities of Quark Amplitudes with Flavor Exchange*, *Nucl.Phys.* **B213** (1983) 122.
- [43] R. Kirschner, *Reggeon interactions in perturbative QCD*, *Z.Phys.* **C65** (1995) 505 [[hep-th/9407085](#)].
- [44] R. Kirschner, *Regge asymptotics of scattering with flavor exchange in QCD*, *Z.Phys.* **C67** (1995) 459 [[hep-th/9404158](#)].
- [45] J. Blumlein and A. Vogt, *On the behavior of nonsinglet structure functions at small x* , *Phys. Lett. B* **370** (1996) 149 [[hep-ph/9510410](#)].
- [46] S. Griffiths and D. Ross, *Studying the perturbative Reggeon*, *Eur.Phys.J.* **C12** (2000) 277 [[hep-ph/9906550](#)].
- [47] Y.V. Kovchegov, D. Pitonyak and M.D. Sievert, *Helicity Evolution at Small- x* , *JHEP* **01** (2016) 072 [[1511.06737](#)].
- [48] Y. Hatta, Y. Nakagawa, F. Yuan, Y. Zhao and B. Xiao, *Gluon orbital angular momentum at small- x* , *Phys. Rev.* **D95** (2017) 114032 [[1612.02445](#)].
- [49] Y.V. Kovchegov, D. Pitonyak and M.D. Sievert, *Helicity Evolution at Small x : Flavor Singlet and Non-Singlet Observables*, *Phys. Rev.* **D95** (2017) 014033 [[1610.06197](#)].
- [50] Y.V. Kovchegov, D. Pitonyak and M.D. Sievert, *Small- x asymptotics of the quark helicity distribution*, *Phys. Rev. Lett.* **118** (2017) 052001 [[1610.06188](#)].
- [51] Y.V. Kovchegov, D. Pitonyak and M.D. Sievert, *Small- x Asymptotics of the Quark Helicity Distribution: Analytic Results*, *Phys. Lett.* **B772** (2017) 136 [[1703.05809](#)].

- [52] Y.V. Kovchegov, D. Pitonyak and M.D. Sievert, *Small- x Asymptotics of the Gluon Helicity Distribution*, *JHEP* **10** (2017) 198 [1706.04236].
- [53] Y.V. Kovchegov and M.D. Sievert, *Small- x Helicity Evolution: an Operator Treatment*, *Phys. Rev.* **D99** (2019) 054032 [1808.09010].
- [54] F. Cougoulic and Y.V. Kovchegov, *Helicity-dependent generalization of the JIMWLK evolution*, *Phys. Rev.* **D100** (2019) 114020 [1910.04268].
- [55] Y.V. Kovchegov and Y. Tawabutr, *Helicity at Small x : Oscillations Generated by Bringing Back the Quarks*, *JHEP* **08** (2020) 014 [2005.07285].
- [56] F. Cougoulic and Y.V. Kovchegov, *Helicity-dependent extension of the McLerran-Venugopalan model*, *Nucl. Phys. A* **1004** (2020) 122051 [2005.14688].
- [57] G.A. Chirilli, *High-energy operator product expansion at sub-eikonal level*, *JHEP* **06** (2021) 096 [2101.12744].
- [58] Y.V. Kovchegov, A. Tarasov and Y. Tawabutr, *Helicity evolution at small x : the single-logarithmic contribution*, *JHEP* **03** (2022) 184 [2104.11765].
- [59] F. Cougoulic, Y.V. Kovchegov, A. Tarasov and Y. Tawabutr, *Quark and Gluon Helicity Evolution at Small x : Revised and Updated*, *JHEP* **07** (2022) 095 [2204.11898].
- [60] A.H. Mueller, *Soft gluons in the infinite momentum wave function and the BFKL pomeron*, *Nucl. Phys.* **B415** (1994) 373.
- [61] A.H. Mueller and B. Patel, *Single and double BFKL pomeron exchange and a dipole picture of high-energy hard processes*, *Nucl. Phys.* **B425** (1994) 471 [hep-ph/9403256].
- [62] A.H. Mueller, *Unitarity and the BFKL pomeron*, *Nucl. Phys.* **B437** (1995) 107 [hep-ph/9408245].
- [63] I. Balitsky, *Operator expansion for high-energy scattering*, *Nucl. Phys.* **B463** (1996) 99 [hep-ph/9509348].
- [64] I. Balitsky, *Factorization and high-energy effective action*, *Phys. Rev.* **D60** (1999) 014020 [hep-ph/9812311].
- [65] Y.V. Kovchegov, *Small- x F_2 structure function of a nucleus including multiple pomeron exchanges*, *Phys. Rev.* **D60** (1999) 034008 [hep-ph/9901281].
- [66] Y.V. Kovchegov, *Unitarization of the BFKL pomeron on a nucleus*, *Phys. Rev.* **D61** (2000) 074018 [hep-ph/9905214].
- [67] J. Jalilian-Marian, A. Kovner and H. Weigert, *The Wilson renormalization group for low x physics: Gluon evolution at finite parton density*, *Phys. Rev.* **D59** (1998) 014015 [hep-ph/9709432].
- [68] J. Jalilian-Marian, A. Kovner, A. Leonidov and H. Weigert, *The Wilson renormalization group for low x physics: Towards the high density regime*, *Phys. Rev.* **D59** (1998) 014014 [hep-ph/9706377].
- [69] H. Weigert, *Unitarity at small Bjorken x* , *Nucl. Phys.* **A703** (2002) 823 [hep-ph/0004044].
- [70] E. Iancu, A. Leonidov and L.D. McLerran, *The renormalization group equation for the color glass condensate*, *Phys. Lett.* **B510** (2001) 133.
- [71] E. Iancu, A. Leonidov and L.D. McLerran, *Nonlinear gluon evolution in the color glass condensate. I*, *Nucl. Phys.* **A692** (2001) 583 [hep-ph/0011241].
- [72] E. Ferreira, E. Iancu, A. Leonidov and L. McLerran, *Nonlinear gluon evolution in the color glass condensate. II*, *Nucl. Phys.* **A703** (2002) 489 [hep-ph/0109115].
- [73] D. Adamiak, Y.V. Kovchegov and Y. Tawabutr, *Helicity evolution at small x : Revised asymptotic results at large N_c and N_f* , *Phys. Rev. D* **108** (2023) 054005 [2306.01651].
- [74] JEFFERSON LAB ANGULAR MOMENTUM (JAM) collaboration, *Global analysis of polarized DIS and SIDIS data with improved small- x helicity evolution*, *Phys. Rev. D* **108** (2023) 114007 [2308.07461].
- [75] S. Moch, J.A.M. Vermaseren and A. Vogt, *The Three-Loop Splitting Functions in QCD: The Helicity-Dependent Case*, *Nucl. Phys. B* **889** (2014) 351 [1409.5131].
- [76] J. Blümlein, P. Marquard, C. Schneider and K. Schönwald, *The three-loop polarized singlet anomalous dimensions from off-shell operator matrix elements*, *JHEP* **01** (2022) 193 [2111.12401].
- [77] Y. Hatta and D.-J. Yang, *On the small- x behavior of the orbital angular momentum distributions in QCD*, *Phys. Lett.* **B781** (2018) 213 [1802.02716].
- [78] J. More, A. Mukherjee and S. Nair, *Wigner Distributions For Gluons*, *Eur. Phys. J. C* **78** (2018) 389 [1709.00943].
- [79] S. Wandzura and F. Wilczek, *Sum Rules for Spin Dependent Electroproduction: Test of Relativistic Constituent Quarks*, *Phys. Lett. B* **72** (1977) 195.
- [80] Y. Hatta and X. Yao, *QCD evolution of the orbital angular momentum of quarks and gluons: Genuine twist-three part*, *Phys. Lett. B* **798** (2019) 134941 [1906.07744].